Techno-Economic and Emission Analysis of Solar Assisted Desiccant Dehumidification System: Experimental and Numerical Approach

By

Wasif Iqbal

Reg # 00000329071

Session 2020-2022

Supervised by

Dr. Mariam Mahmood

MASTER OF SCIENCE in

Thermal Energy Engineering

**U.S-Pakistan Center for Advanced Studies in Energy (USPCAS-E)**

National University of Sciences and Technology (NUST)

H-12, Islamabad 44000, Pakistan

May 2023

THESIS ACCEPTANCE CERTIFICATE

Certified that final copy of MS/MPhil thesis written by Wasif Iqbal (Registration No. 00000329071), of U.S.-Pakistan Centre for Advanced Studies in Energy has been vetted by undersigned, found complete in all respects as per NUST Statues/Regulations, is within the similarity indices limit and accepted as partial fulfillment for the award of MS/MPhil degree. It is further certified that necessary amendments as pointed out by GEC members of the scholar have also been incorporated in the said thesis.

Signature: _____

Name of Supervisor: Dr. Mariam Mahmood

Date: 21-06-2023

Signature (HoD): _____

Date: _____

Signature (Dean/Principal): _____

Date: _____

Certificate

This is to certify that work in this thesis has been carried out by **Mr. Wasif Iqbal** and completed under my supervision in, US-Pakistan Center for Advanced Studies in Energy (USPCAS-E), National University of Sciences and Technology, H-12, Islamabad, Pakistan.

Supervisor:
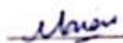
Dr. Mariam Mahmood
USPCAS-E
NUST, Islamabad

GEC member 1:
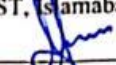
Dr. Adeel Waqas
USPCAS-E
NUST, Islamabad

GEC member 2:
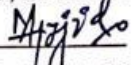
Dr. Majid Ali
USPCAS-E
NUST, Islamabad

GEC member 3:
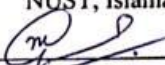
Dr. Mustafa Anwar
USPCAS-E
NUST, Islamabad

HOD-TEE:
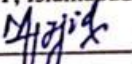
Dr. Majid Ali
USPCAS-E
NUST, Islamabad

Dean/Principal:
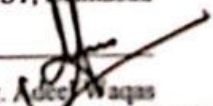
Dr. Adeel Waqas
USPCAS-E
NUST, Islamabad

Dedication

To my dear parents, (Mr. Asif Iqbal and Ms. Zohra Yasmeen) as well as my sister, who have always encouraged me to pursue my goals and motivated me to believe in myself; without their unwavering support, the completion of this project would not have been possible.

Abstract

In humid climates, it is challenging to maintain the amount of moisture content in the air for human thermal comfort and industrial applications. Regeneration is an essential process during moisture removal through a desiccant dehumidifier. Commercial desiccant dehumidifiers rely on conventional electric heaters to regenerate desiccant material, accounting for significant energy consumption by such systems. As a green solution to this problem, the present study integrates a flat plate solar air collector (FPSAC) with a desiccant dehumidifier to effectively use solar thermal energy and reduce electrical consumption. Performance evaluation of glazed and unglazed FPSAC-assisted desiccant dehumidifier has been conducted at process air flow rates of 33, 51 and 62 m^3/h with a constant regeneration flow rate of 42 m^3/h. Both glazed and unglazed FPSAC assisted desiccant dehumidification systems had the highest dehumidification effectiveness and percentage increase in temperature at the flow rate of 33 m^3/h, while the highest moisture removal capacity was at 51 m^3/h. Maximum dehumidification effectiveness, percentage temperature increase, and moisture removal capacity for the glazed case were 0.4, 66.67%, and 6.14 kg/h, respectively. Experimental results showed that the glazed FPSAC-integrated desiccant dehumidification system outperforms its counterpart in all performance evaluation parameters. Using Transient System Simulation software (TRNSYS), the proposed glazed and unglazed assisted desiccant dehumidification system was modeled and validated with experimental results in terms of regeneration inlet temperature, process air outlet relative humidity, and process air outlet temperature at a flow rate of 33 m^3/h. Furthermore, a techno-economic analysis of the solar hybrid desiccant dehumidification system has been carried out. The FPSAC used in this study showcased a 33.57% yearly solar fraction with a solar hybrid system having a payback period of 7.28 years with gasoline as a fuel source for auxiliary energy. In addition, the hybrid system can reduce greenhouse gas emissions yearly by about 0.352 tonnes of CO_2 equivalents.

Keywords: Solar air collector, desiccant dehumidifier, rotary desiccant wheel, TRNSYS simulation, economic feasibility, CO_2 emissions.

Table of Contents

List of Figures

List of Tables

List of Publications

1. Wasif Iqbal, Mariam Mahmood, Adeel Waqas, Naveed Ahmed, Muhammad Haroon Iqbal, "Techno-Economic and Emission Analysis of Solar Assisted Desiccant Dehumidification System: Experimental and Numerical Approach," *Sustainable Energy Technologies and Assessment*, 2023. (Submitted)

2. Wasif Iqbal, Mariam Mahmood, Adeel Waqas, Majid Ali, Naveed Ahmed, Muhammad Haroon Iqbal, "Performance Evaluation of Solar Assisted Desiccant Dehumidification System," 2nd *International Conference on Emerging Power Technologies (ICEPT), IEEE,* 2023. (Presented)

Chapter 1

Introduction

1.1. Background

An imbalance between energy availability and demand for energy has been generated by rapidly expanding populations and enormous industrial growth. Even though they have significant negative effects on human health and the environment, fossil fuels remain the primary energy source [1][2]. During the course of the last few years, there has been an increase in the need for energy on a global scale. The global energy demand is set to rise by 50% by the 2050s [3]. To meet this demand, fossil fuels are burned, depleting natural resources and causing detrimental effects on human health and the environment [4]. A country must rely less on non-renewable energy sources (gas, coal, and oil) and more on efficiently using renewable energy resources to ensure long-term energy security [5]. Pakistan's energy demand is rapidly increasing, like that of other countries. Domestic and industrial sectors require increasing energy to meet their needs. At the moment, this demand is mostly met by burning fossil fuels, which not only depletes existing reserves of fossil fuels in the country and leads to a shortage of energy but also has a negative impact on the environment and health. Electrical energy shortfall is also a serious concern for the country's economic growth. In 2020 electricity generation stood at 22 GW against the peak demand of 25 GW. However, the actual peak demand ratio is increasing annually [6]. There is an imperative need for the current energy mix to undergo an immense transition. Renewable energy in all its forms is indispensable when reconciling rising energy needs with long-term prosperity [7]. The global renewable energy scenario by 2040 is presented in **Tabl.1.**

Table 1.1 Global renewable energy scenario by 2040 [8]

	2001	2010	2020	2030	2040
Total consumption (million tons oil equivalent)	10,038	10,549	11,425	12,352	13,310
Solar Thermal Electricity	0.1	0.4	3	16	68
Photovoltaic	0.1	2	24	221	784
Large Hydro	22.7	206	309	341	358
Small Hydro	9.5	19	49	106	189
Biomass	1080	1313	1791	2483	3271
Geothermal	43.2	86	186	333	493
Wind	4.7	44	266	542	688
Marine (tidal/wave/ocean)	0.05	0.1	0.4	3	20
Total RES	1365.5	1745.5	2964.4	4289	6351
Renewable energy source contribution (%)	13.6	16.6	23.6	34.7	47.7

Solar energy is abundant in renewable energy sources and has vast reserves. However, according to statistics, solar energy accounts for less than 1.0% of the world's primary energy supply [9]. As a result of its significant application potential, solar-thermal energy has gained increasing attention. When solar energy is directed at a FPSAC, it can be used for space heating, dehumidification, desalination, and many other domestic and industrial applications [10].

1.2. Dehumidification of air

Humidity plays a vital role in different areas of life including human thermal comfort, industrial, pharmaceutical, and food production and storage industries [11]. Also, electronic production facilities require a relatively low humidity range (for surface mounted technology requires 40~45% relative humidity) for precise and high-quality manufacturing [12]. Hot and humid climatic areas contain a large amount of water content in the air and it requires the removal of water from the air so that the dehumidified air can be used for human thermal comfort, power plants, cold storage industries, and domestic and industrial applications [13]. An efficient dehumidification system helps in the betterment of people and industrial growth.

Generally, dehumidification of air can be done by the following methods:

1. Cooling Condensation
2. Electrically Driven Dehumidification (EDD)
3. Desiccant Dehumidification

1.2.1. Cooling Condensation

A vapor compression cooling system is the most commonly used cooling condensation system. Vapor is compressed and turned into liquid throughout this cycle. To enable fluid to evaporate at low pressure, the pressure is kept low. But there is some limitation to using a vapor compression cooling system such as insufficient dehumidification capacity, due to moist cooling coils resulting in mild dew and bacteria formation and electrical malfunction [14]. There is another cooling condensation method for dehumidification called thermoelectric cooling dehumidification in which air is cooled by Peltier effect and then pass through the electric field for dehumidification [15]. But the problem with this approach of dehumidification. Sometimes after dehumidification air has to be preheat to meet the desired temperature requirement and because of this heating and cooling this method of dehumidification becomes quite expensive [16].

1.2.2. Electrically Driven Dehumidification

In EDD, water is removed from the air by electrolysis. During electrolysis process when electric field is applied hydrated water molecules charge up and the migration of anions

and cations starts. This results the separation of ions and water [11]. Working principal of EDD is shown in the **Fig. 1.1.**
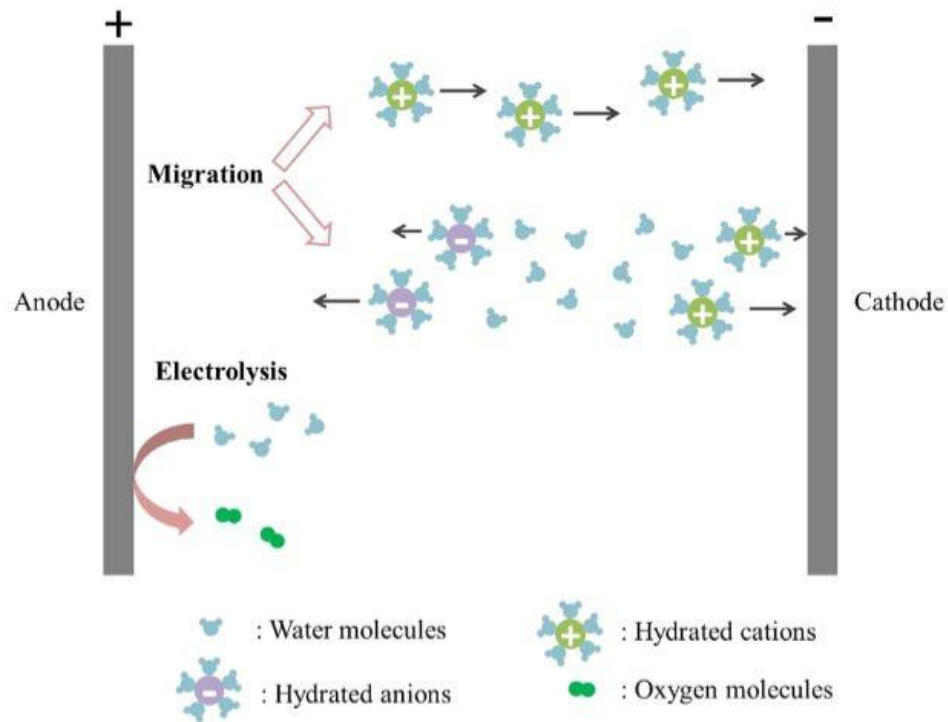
Fig. 1.1 Schematic of EDD

1.2.3. Desiccant Dehumidification

Dehumidification of air through desiccant systems were first introduced in 1930s [17]. Desiccants are the materials that can absorb moisture from air by the phenomenon of vapor pressure difference between the supplying air and the desiccant surface. The process of transfer of moisture from ambient air to the desiccant surface occurs continuously until the vapor pressure of desiccant surface is lower than the surrounding air. When the desiccant surface or desiccant material reaches equilibrium condition and becomes saturated, transfer of moisture from air to desiccant surface stops. Now to remove the moisture from the desiccant surface and make it possible to use it again, a regeneration process is used which carry out the moisture of it. Regeneration can be done either by absorption or absorption. In absorption chemical or physical change occurs in a desiccant material while adsorption leads to no physical or chemical change rather than it take place on the desiccant surface [18].

4

Desiccant materials can be liquid or solid. The absorption process for liquid desiccants is carried out by a deliquescent material such as calcium chloride ($CaCl_2$) and lithium chloride. On the other hand, the absorption process for solid desiccants can be carried out by either a polymer sorbent or a porous material such as silica gel, alumina silicate, and zeolite [19].

Following are the configurations of desiccant based dehumidification.

1.2.3.1. Packed Bed

In packed or fixed-bed systems, granules of desiccant are packed tightly into a bed that stays in one place. The dehumidification and regeneration modes can be reached by switching between the process airflow and the regeneration airflow over the bed. The main benefit of fixed-bed systems is that they are easy to set up and make. On the other hand, because the flowing gas and the desiccant don't contact each other very much, the average coefficients of heat and mass transfer are low. Also, the high turbulent flow of the process air causes the airflow pressure drop to rise unnecessarily, which uses more power [20]. The experimental design of examining the multilayer bed is shown in **Fig. 1.2.**
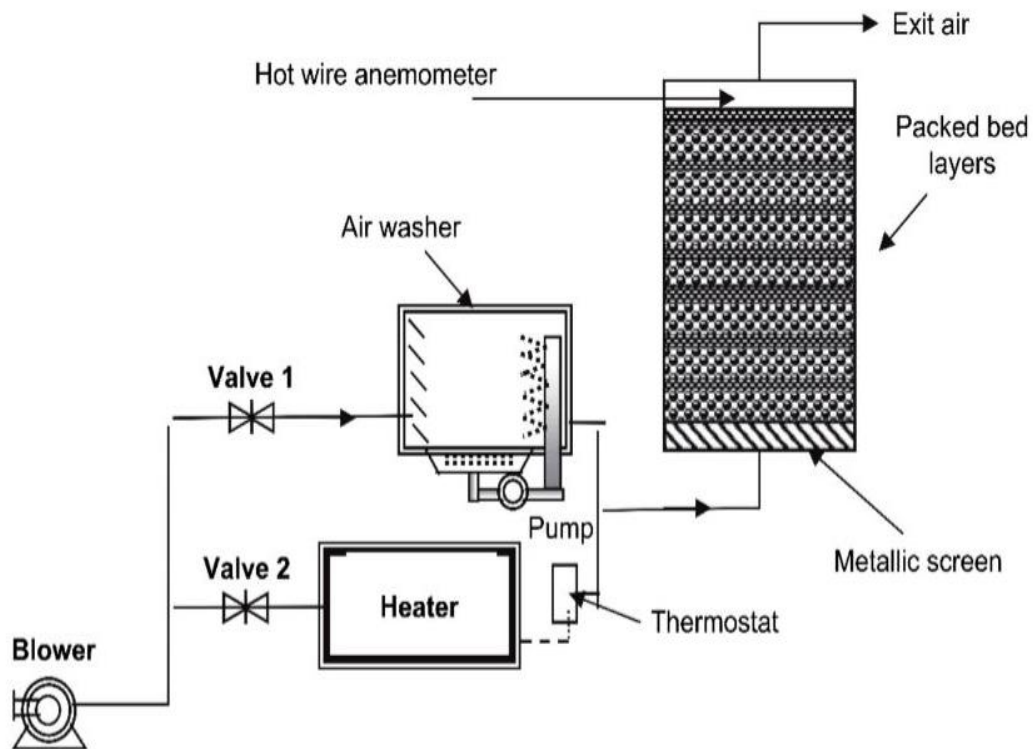
Fig. 1.2 Experimental design of multilayer packed bed

1.2.3.2. Fluidized Bed

A desiccant bed configuration known as a packed bed generates the desiccant substance by simply packing it into the bed. This facilitates simple and inexpensive production. Unfortunately, this configuration has a significant pressure drop and a low usage rate of the desiccant, which are major causes for concern. Fluidized beds, on the other hand, allow the desiccant material to move freely and simply circulate within the bed itself, resulting in a reasonable efficiency in both mass and heat transfer as well as a low-pressure drop. An overview of the silica gel fluidized bed system with a schematic representation is shown in **Fig.1.3.** [21].
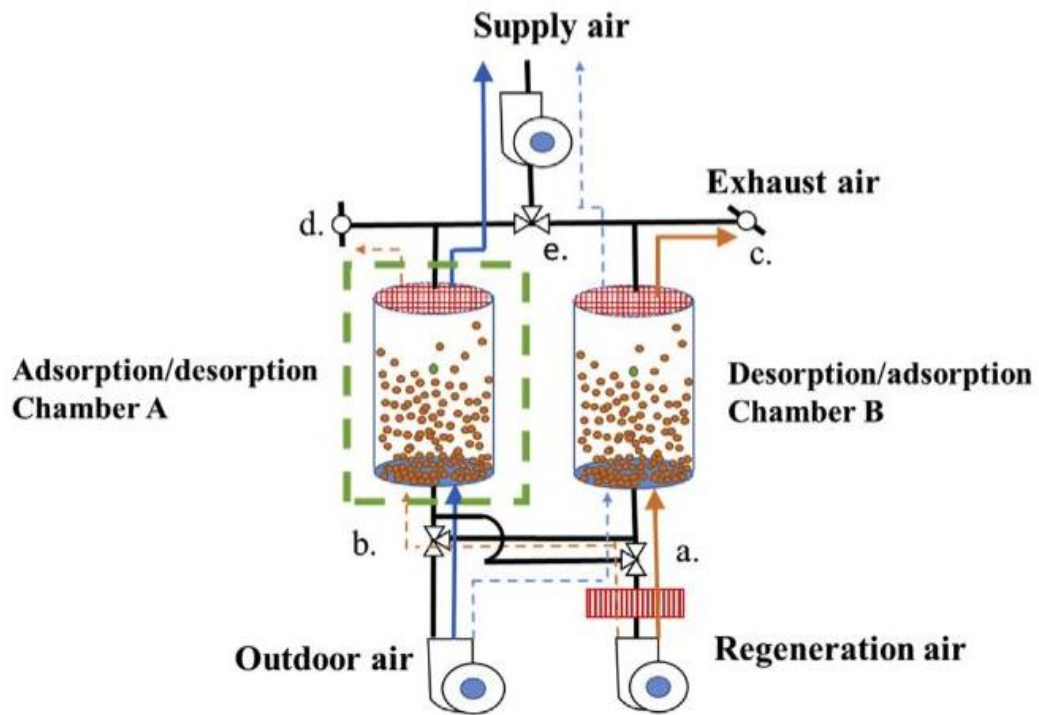
Fig. 1.3 Schematic of fluidized packed bed

1.2.3.3. Rotary Desiccant Wheel

The revolving wheel that is a part of a solid desiccant cooling system is considered one of the system's most important components. It has a major impact on both its productivity and its price. Controlling moisture and maximizing enthalpy recovery are its primary responsibilities. The rotary desiccant wheel dehumidifiers have several advantages over other dehumidifying configurations, such as their ability to create a continuous cycle, relative compactness, higher efficiency, and potential to acquire the required regeneration heat from low-grade sources, such as solar energy and waste heat. Additionally, these dehumidifiers are more cost-effective. As a consequence of this, spinning desiccant wheel dehumidifiers are an excellent alternative to dehumidification technology from the perspective of energy efficiency. Schematic of rotary desiccant wheel dehumidification system is shown [22].
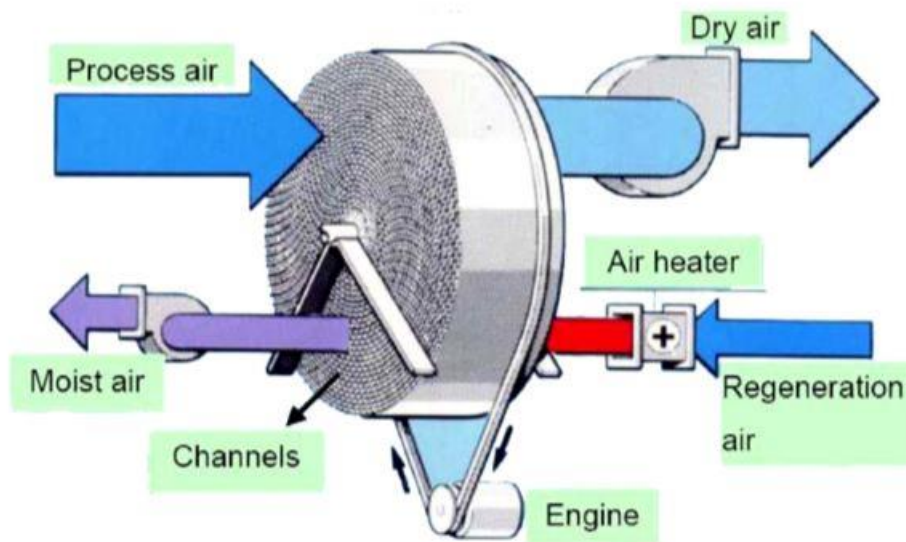
Fig. 1.4 Schematic of rotary desiccant wheel system

1.3. Scope and Limitations

1.3.1. Scope

In this study, experimental analysis was done on the desiccant dehumidification system by integrated with glazed and unglazed solar air collector at different process air flow rates. TRNSYS model is developed and validated with experimental results with best agreement. Moreover, emission and economic analysis is done for solar hybrid desiccant dehumidification system.

1.3.2. Limitations

The experimental prototype was designed for a lab-scale; therefore, the operating capacity of the components was limited.

1.4. Organization of thesis

Chapter 1
- Provides information on how the use of fossil fuels affecting the climate.
- Provides information on the use of renewable energy for sustaniable growth.
- Provides information on the importance of dehumidification of air and its techniques.

Chapter 2
- Thorough analysis of lityerature review.
- Discuss different types of configurations of rotary desiccant system.

Chapter 3
- Discuss detailed methodolgy and experimental setup of proposed system.
- Numerical equations to analyze the performance of SADDS.
- Detailed discussion on the TRNSYS model of the proposed system.

Chapter 4
- Detailed analysis on the experiemntal results of glazed and unglazed solar air collector assisted desiccant dehumidification system.
- Disussion on the dehumidification effectiveness, moisture removal capacity, percentage increase in temperature for both glazed and unglazed cases.
- Validation of TRNSYS model with experimental results.
- Carbon emission and financial assessment of the proposed system.

Chapter 5
- Discusses the objectives, methodology and obtained results.
- Discusses the possible future prospects in this study.

Fig. 1.5 Thesis flow chart

Summary

The necessity of shifting away from traditional energy sources and toward renewable energy sources is discussed in this chapter. In addition to this, the significance of removing the moisture content from the air as well as the many methods that may be used to achieve this objective, is also covered.

References

[1]   X. Yang, J. Pang, F. Teng, R. Gong, and C. Springer, "The environmental co-benefit and economic impact of China's low-carbon pathways: Evidence from linking bottom-up and top-down models," *Renew. Sustain. Energy Rev.*, vol. 136, no. October 2020, p. 110438, 2021, doi: 10.1016/j.rser.2020.110438.

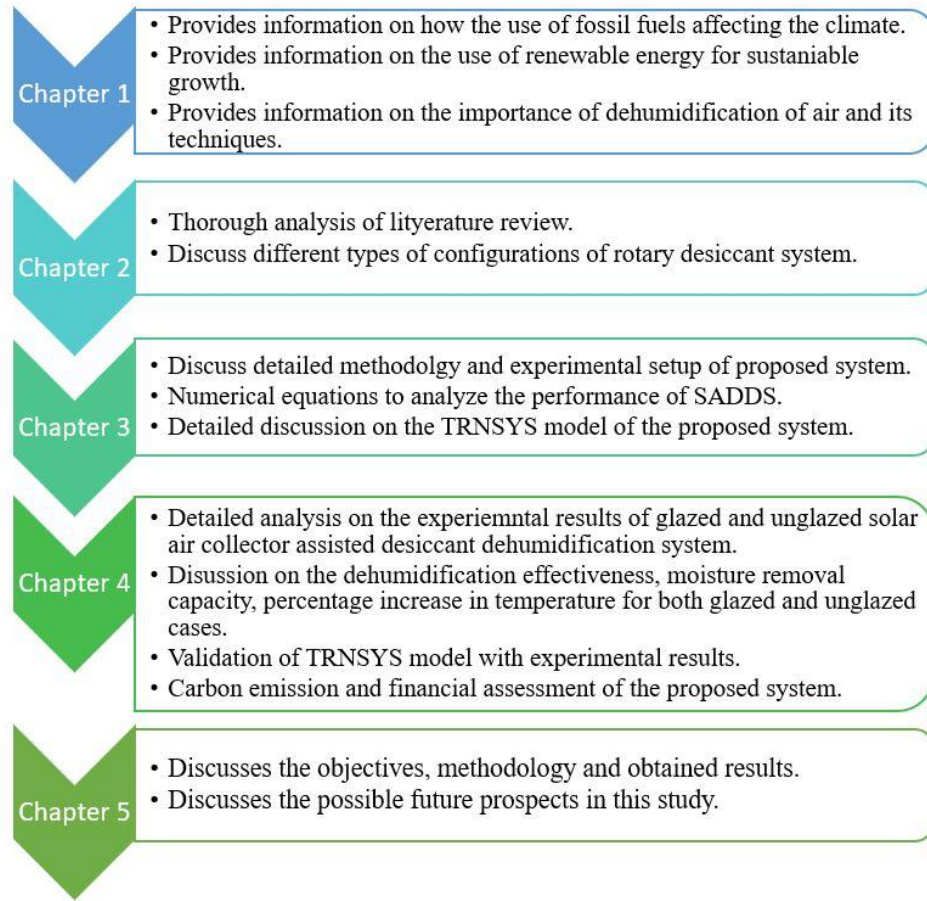[2]   J. Curtin, C. McInerney, B. Ó Gallachóir, C. Hickey, P. Deane, and P. Deeney, "Quantifying stranding risk for fossil fuel assets and implications for renewable energy investment: A review of the literature," *Renew. Sustain. Energy Rev.*, vol. 116, no. September, p. 109402, 2019, doi: 10.1016/j.rser.2019.109402.

[3]   P. Vivekh, S. D. Pei, W. Pang, and G. Cheng, "Air dehumidification performance study of a desiccant wheel by a three-dimensional mathematical model," *Int. J. Refrig.*, 2022, doi: 10.1016/j.ijrefrig.2022.10.011.

[4]   A. Demirbaş, "Biomass resource facilities and biomass conversion processing for fuels and chemicals," *Energy Convers. Manag.*, vol. 42, no. 11, pp. 1357–1378, 2001, doi: 10.1016/S0196-8904(00)00137-0.

[5]   Z. Nawaz, N. Ramzan, S. Nawaz, S. Naveed, and M. Bilal Khan, "Green processing of coal to liquid fuels: Pakistan's perspective," *Proc. Pakistan Acad. Sci.*, vol. 49, no. 3, pp. 165–172, 2012.

[6]   J. Tao, M. Waqas, M. Ali, M. Umair, W. Gan, and H. Haider, "Pakistan's electrical energy crises, a way forward towards 50% of sustain clean and green electricity generation," *Energy Strateg. Rev.*, vol. 40, p. 100813, 2022, doi: 10.1016/j.esr.2022.100813.

[7]   M. K. Abdelrazik, S. E. Abdelaziz, M. F. Hassan, and T. M. Hatem, "Climate action: Prospects of solar energy in Africa," *Energy Reports*, vol. 8, pp. 11363–11377, 2022, doi: 10.1016/j.egyr.2022.08.252.

[8]   I. Kralova and J. Sjöblom, "Biofuels-renewable energy sources: A review," *J. Dispers. Sci. Technol.*, vol. 31, no. 3, pp. 409–425, 2010, doi: 10.1080/01932690903119674.

[9]   J. Zhang and T. Zhu, "Systematic review of solar air collector technologies:

Performance evaluation, structure design and application analysis," *Sustain. Energy Technol. Assessments*, vol. 54, no. 409, p. 102885, 2022, doi: 10.1016/j.seta.2022.102885.

[10] E. Vengadesan and R. Senthil, "A review on recent developments in thermal performance enhancement methods of flat plate solar air collector," *Renew. Sustain. Energy Rev.*, vol. 134, no. August, p. 110315, 2020, doi: 10.1016/j.rser.2020.110315.

[11] H. Liu, H. Yang, and R. Qi, "A review of electrically driven dehumidification technology for air-conditioning systems," *Appl. Energy*, vol. 279, no. September, p. 115863, 2020, doi: 10.1016/j.apenergy.2020.115863.

[12] Y. Fang and L. Tan, "The intelligent SMT workshop monitoring system based on ZigBee wireless sensor network," *Proc. - 2013 Int. Conf. Comput. Sci. Appl. CSA 2013*, pp. 150–153, 2013, doi: 10.1109/CSA.2013.41.

[13] U. Eicker *et al.*, "Experimental investigations on desiccant wheels," *Appl. Therm. Eng.*, vol. 42, pp. 71–80, 2012, doi: 10.1016/j.applthermaleng.2012.03.005.

[14] A. T. Mohammad, S. Bin Mat, M. Y. Sulaiman, K. Sopian, and A. A. Al-Abidi, "Survey of hybrid liquid desiccant air conditioning systems," *Renew. Sustain. Energy Rev.*, vol. 20, pp. 186–200, 2013, doi: 10.1016/j.rser.2012.11.065.

[15] R. Qi, D. Li, and L. Z. Zhang, "Performance investigation on polymeric electrolyte membrane-based electrochemical air dehumidification system," *Appl. Energy*, vol. 208, no. May, pp. 1174–1183, 2017, doi: 10.1016/j.apenergy.2017.09.035.

[16] G. A. Longo and A. Gasparella, "Experimental and theoretical analysis of heat and mass transfer in a packed column dehumidifier / regenerator with liquid desiccant," vol. 48, pp. 5240–5254, 2005, doi: 10.1016/j.ijheatmasstransfer.2005.07.011.

[17] M. Shehadi, "Review of humidity control technologies in buildings," *J. Build. Eng.*, vol. 19, pp. 539–551, 2018, doi: 10.1016/j.jobe.2018.06.009.

[18] S. Jain and P. K. Bansal, "Performance analysis of liquid desiccant dehumidification systems," *Int. J. Refrig.*, vol. 30, no. 5, pp. 861–872, 2007, doi: 10.1016/j.ijrefrig.2006.11.013.

[19]   S. Misha, S. Mat, M. H. Ruslan, and K. Sopian, "Review of solid/liquid desiccant in the drying applications and its regeneration methods," *Renew. Sustain. Energy Rev.*, vol. 16, no. 7, pp. 4686–4707, 2012, doi: 10.1016/j.rser.2012.04.041.

[20]   X. N. Wu, T. S. Ge, Y. J. Dai, and R. Z. Wang, "Review on substrate of solid desiccant dehumidification system," *Renew. Sustain. Energy Rev.*, vol. 82, no. July 2017, pp. 3236–3249, 2018, doi: 10.1016/j.rser.2017.10.021.

[21]   C. H. Chen, G. Schmid, C. T. Chan, Y. C. Chiang, and S. L. Chen, "Application of silica gel fluidised bed for air-conditioning systems," *Appl. Therm. Eng.*, vol. 89, pp. 229–238, 2015, doi: 10.1016/j.applthermaleng.2015.05.058.

[22]   M. M. Abd-Elhady, M. S. Salem, A. M. Hamed, and I. I. El-Sharkawy, "Solid desiccant-based dehumidification systems: A critical review on configurations, techniques, and current trends," *Int. J. Refrig.*, vol. 133, no. February 2021, pp. 337–352, 2022, doi: 10.1016/j.ijrefrig.2021.09.028.

Chapter 2

Literature Review

Pakistan's energy demand is rapidly increasing, like that of other countries. Domestic and industrial sectors require increasing energy to meet their needs. At the moment, this demand is mostly met by burning fossil fuels, which not only depletes existing reserves of fossil fuels in the country and leads to a shortage of energy but also has a negative impact on the environment and health. Electrical energy shortfall is also a serious concern for the country's economic growth. In 2020 electricity generation stood at 22 GW against the peak demand of 25 GW. However, the actual peak demand ratio is increasing annually [1]. There is an imperative need for the current energy mix to undergo an immense transition. In its various forms, renewable energy plays a vital role in bridging the gap between increased energy demand and sustainable growth.

Removal of moisture from the air is critical in many aspects of life, including human thermal comfort, industrial, pharmaceutical, and food production and storage. Furthermore, for precise and high-quality manufacturing, electronic manufacturing facilities require a relatively low humidity range (40-45% relative humidity for surface-mounted technology) [2][3]. Dehumidification of moist air contributes to improved human thermal comfort and industrial growth.

2.1. Rotary Desiccant Dehumidification System

Rotary desiccant wheel-based dehumidification system has been extensively studied. To name a few of these, Su et al. [4] investigated the performance of dehumidification when combined with precooling and a recirculated regenerative rotor desiccant wheel. Total moisture removal capacity (MRC_{tot}) and thermal coefficient of performance are key performance indicators (COP_{th}). It was found that the proposed system's MRC_{tot} improved by 29.7% compared to the conventional cooling system. The COP_{th} of the system increased by increasing process airflow temperature or humidity and decreasing precooling temperature.

14
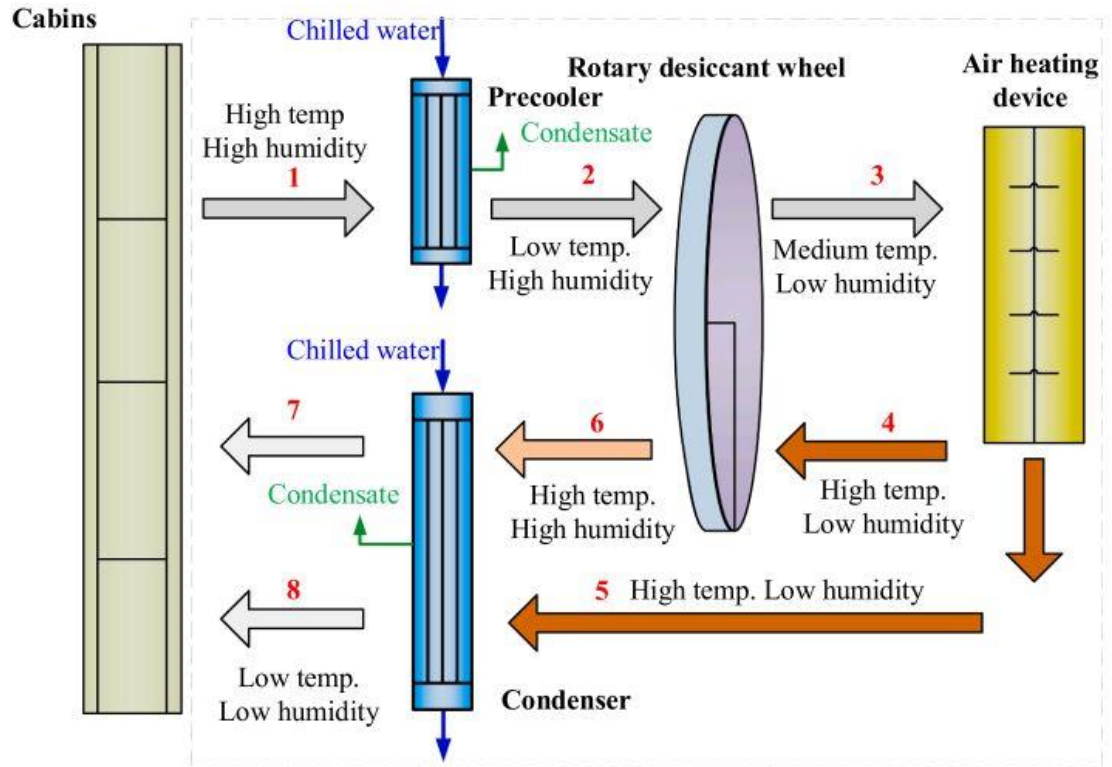
Fig. 2.1. Working principle of the dehumidification system integrated with precooling and recirculated regenerative rotary desiccant wheel

Saputra et al. [5] examined the desiccant wheel effectiveness for two operating modes, i.e., constant regeneration temperature with varying regeneration air velocity and constant regeneration air velocity with varying regeneration temperature. Results confirmed that the desiccant wheel performs better at constant regeneration temperature as compared to the constant regeneration air velocity.
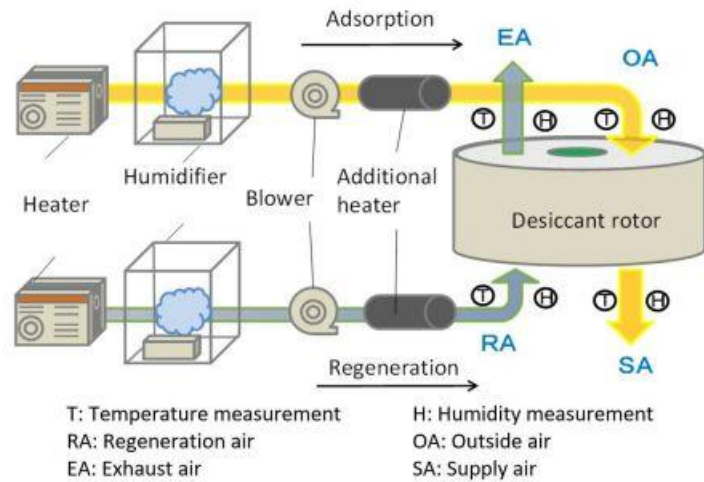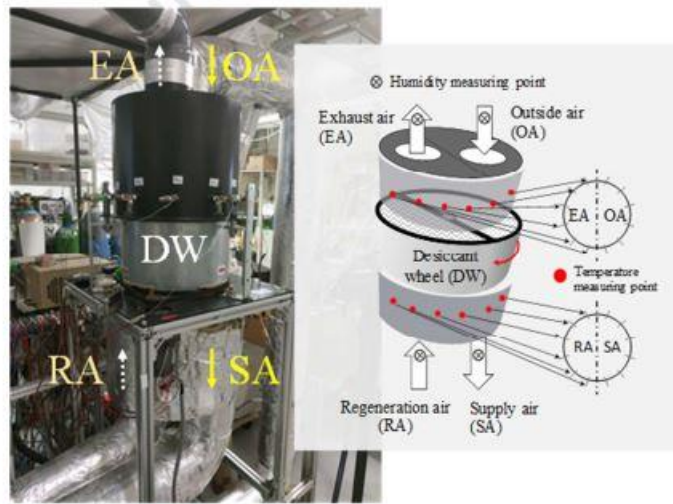
Fig. 2.2. (a) Schematic diagram and (b) photographic view of the experimental apparatus.

Researchers Ge et al. [6] studied the performance of a two-stage rotary desiccant cooling system using a combination of regeneration temperatures. Performance was evaluated by calculating COP_{th} and cooling capacity. The computed findings showed that the COP_{th} of the system drops when the regeneration temperature rises in response to an increase in cooling power. It was also found that when the first stage operated at a greater regeneration temperature than the second stage, the COP_{th} and cooling power were enhanced.
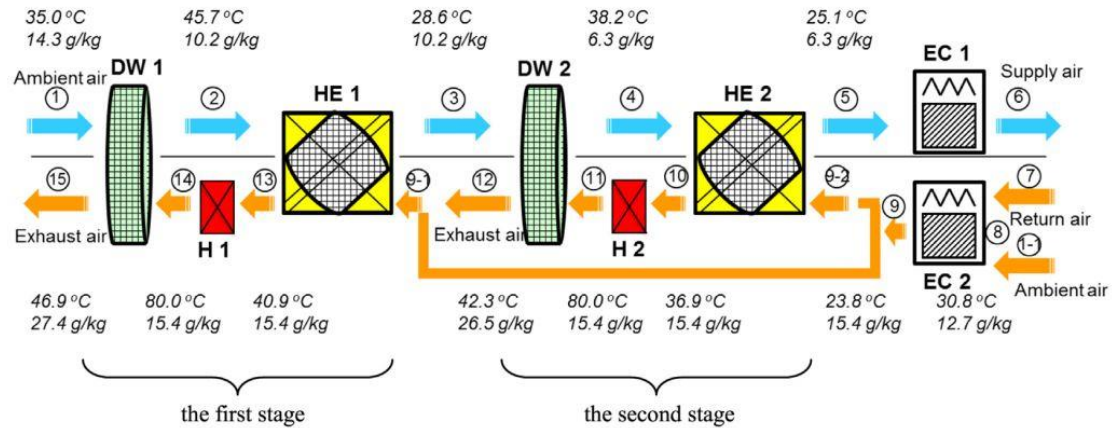
Fig.2.3. Schematic figure of two-stage rotary wheel desiccant cooling system

Angrisani et al. [7] conducted an experimental analysis of the rotary desiccant wheel performance. The results showed that the process air humidity ratio and regeneration temperature significantly influence dehumidification performance more than process air temperature and regeneration air flow rate. Comino et al. [8] also analyzed the performance of a desiccant wheel by altering its rotational speed and measuring temperature and humidity at 32 different circular cross-sections of the wheel. The results showed that decreasing the rotational speed reduces the temperature of the desiccant material on the process side while increasing the temperature on the regeneration side. It was also observed that the circular sectors closest to the regeneration side had the maximum process side air dehumidification while experiencing the least increase in outlet temperature.

Chai et al. [9] combined the desiccant system with a heat pump, which directed the rejected heat from the air conditioning system to the desiccant-coated heat exchanger for regeneration. When compared to the conventional condensation dehumidification system, the COP of the proposed system is improved by 13-40%. The moisture removal per kilowatt hour electric power consumption is 1.60-2.88 times greater than that of conventional condensation dehumidification system. Desiccant material is critical in desiccant dehumidification, and the desiccant material should be chosen based on its high adsorption capacity.
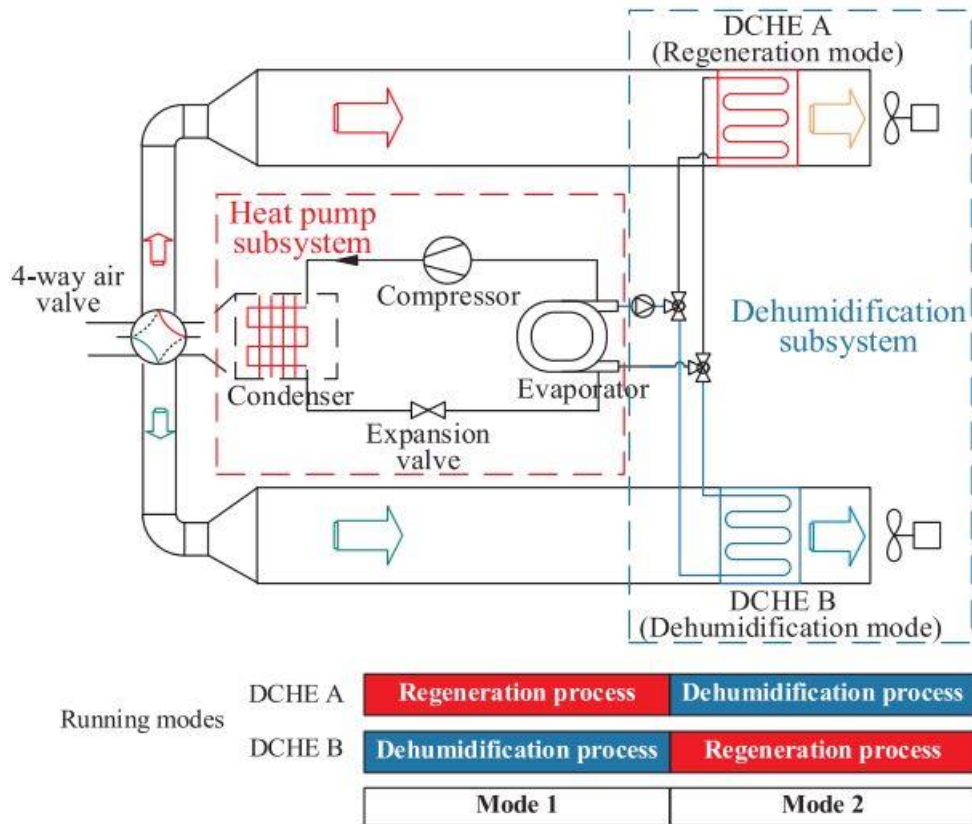
17

Fig. 2.4. Schematic of the fresh air heat pump dehumidification system

Jacob et al. [10] investigated the adsorption capacity of various pour-size silica gels over 5000 temperature swing adsorption cycles at 250 °C regeneration temperature. It was observed that silica gel with larger porous sizes loses less adsorption capacity than silica gel with smaller pores. Behede et al. [11] synthesized the nanoporous inorganic desiccant material, i.e., aerogels, aluminophosphate-based molecular sieves, and aluminosilicate zeolites. According to the findings, this class of desiccant has a high adsorption capacity compared to conventional desiccant materials (silica gel, zeolites, activated carbon, etc.). Jia et al. [12] experimentally compared the two desiccant wheels having one silica gel and other composite material, i.e., LiCl, as a desiccant material. Results showed that composite material removes 50% more moisture from the humid air than the silica gel.

Specifically, in line with the objectives and scope of this study, several studies have been conducted on the integration of solar collector with the rotary desiccant system. TRNSYS simulation was used by Fong et al. [13] to optimize the solar-powered desiccant wheel

18
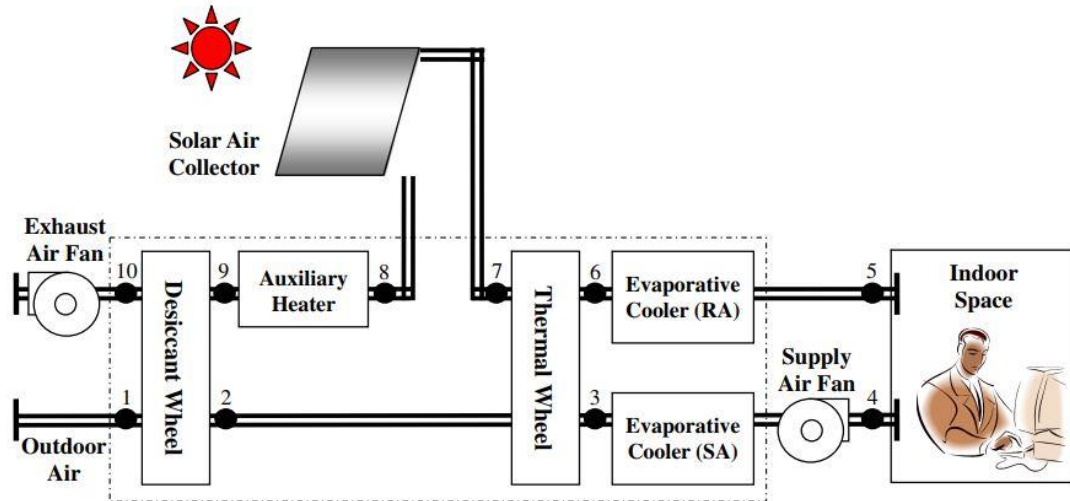
Fig. 2.5. Schematic diagram of solar-assisted desiccant cooling system

evaporative cooling system (SPDCS) for Hong Kong's subtropical environment. Solar fraction and coefficient of performance were assessed using SADC's optimal design. The monthly average solar fraction was 8% to 33%, while the yearly average was 17%. COP ranged from 1.08 to 1.60 per month, with a mean of 1.38. SADCS proved to be a viable alternative to refrigeration air-conditioning. Misha et al. [14] investigated the solar-assisted rotary desiccant system for drying kenaf core fiber. After two days of drying, the moisture level in five random kenaf trays was less than 18%. Compared to open sun drying, the drying time required to remove moisture below 18% from kenaf fiber was reduced from 20.75 h to 15.75 h.
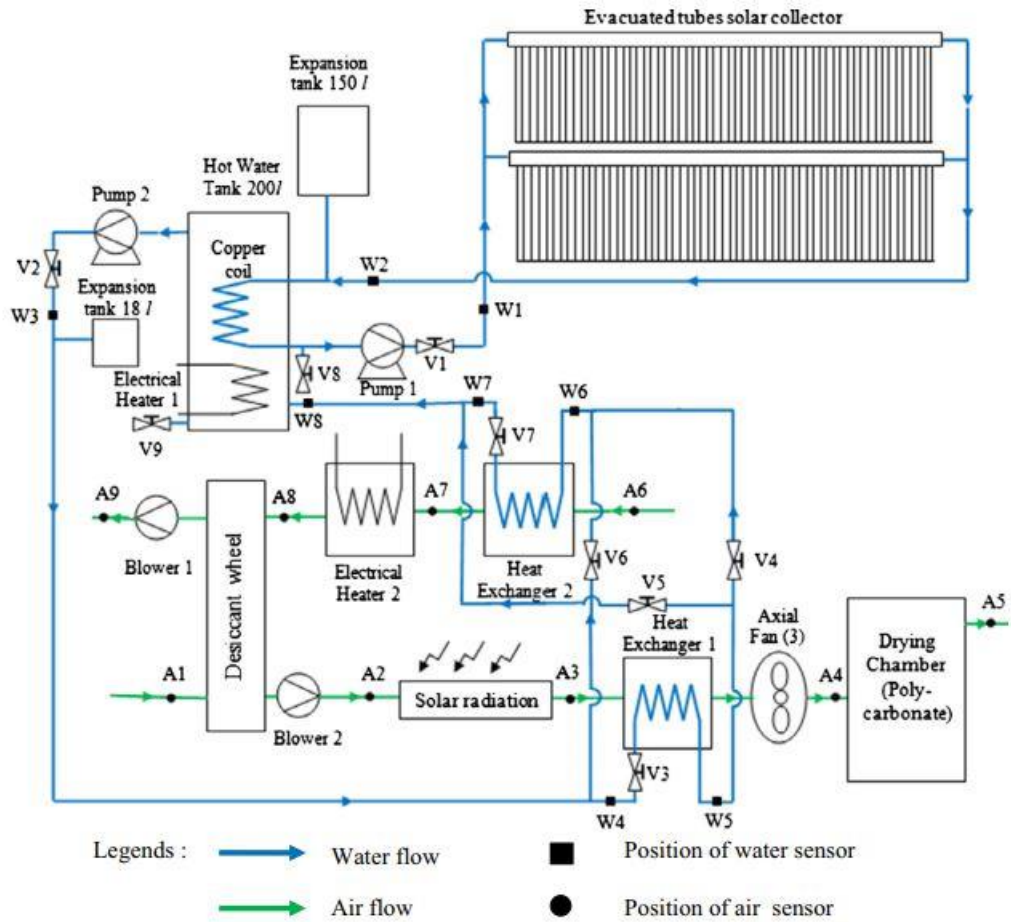
Fig. 2.6. Schematic diagram of the experimental setup

The effect of dry bulb temperature on the solar-driven hybrid rotary desiccant system was investigated by Jani et al. [15] through experimentation and simulation. Evidence suggests that the process-side adsorption rate drops as dry bulb temperature (DBT) rise. Adsorption rates can be raised by elevating the regeneration temperature. It was also observed that the dehumidification efficiency and moisture removal rate increased with increasing regeneration temperature as the dry DBT increased.
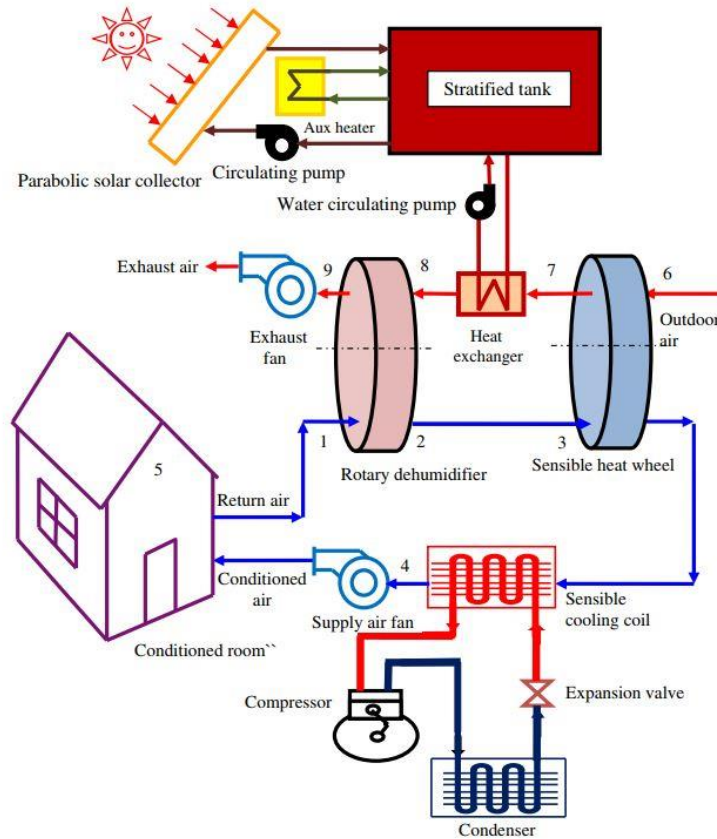
Fig. 2.7. Working diagram of solar-integrated solid-desiccant-coupled thermally activated hybrid comfort space conditioning system

Dezfouli et al. [16] simulated the two-stage solar desiccant cooling system for energy-efficient Malaysian buildings using TRNSYS. In ventilation and recirculation mode, the system could bring the temperature and relative humidity to 25.5°C–25°C and 61%–66%, respectively. Energy savings for ventilation and recirculation were 27.9% and 33.9%, respectively. The monthly CO2 emission was lowered to 256.4 Kg. %. Li at el. [17] did the energy and economic analysis of a solar-assisted desiccant dehumidification system combined with a conventional air conditioning system. The results demonstrated that the proposed system could save 6,760 kWh of energy with an approximate 7-year payback period. Ahmed et al. [18] performed the computational and experimental analysis to optimize the desiccant wheels' performance. At a flow rate of 1.9 kg/min, a 2m^2 solar air collector can provide 72.8% of the total energy required for regeneration, whereas, at a flow rate of 9.4 kg/min, this figure reduces to 13.7%.

Summary

The rotary desiccant wheel-based dehumidification system has been extensively studied, focusing on performance improvement and optimization. Various factors such as precooling, regeneration temperature, airflow, and desiccant material have been investigated. Studies have shown that the proposed systems exhibits significant enhancements in moisture removal capacity and thermal coefficient of performance compared to conventional cooling systems. Integration of solar collectors with the desiccant system has also been explored, demonstrating its viability as an alternative to refrigeration air-conditioning and achieving energy savings.

References

[1]   J. Tao, M. Waqas, M. Ali, M. Umair, W. Gan, and H. Haider, "Pakistan's electrical energy crises, a way forward towards 50% of sustain clean and green electricity generation," *Energy Strateg. Rev.*, vol. 40, p. 100813, 2022, doi: 10.1016/j.esr.2022.100813.

[2]   H. Liu, H. Yang, and R. Qi, "A review of electrically driven dehumidification technology for air-conditioning systems," *Appl. Energy*, vol. 279, no. September, p. 115863, 2020, doi: 10.1016/j.apenergy.2020.115863.

[3]   Y. Fang and L. Tan, "The intelligent SMT workshop monitoring system based on ZigBee wireless sensor network," *Proc. - 2013 Int. Conf. Comput. Sci. Appl. CSA 2013*, pp. 150–153, 2013, doi: 10.1109/CSA.2013.41.

[4]   M. Su, X. Han, D. Chong, J. Wang, J. Liu, and J. Yan, "Experimental study on the performance of an improved dehumidification system integrated with precooling and recirculated regenerative rotary desiccant wheel," *Appl. Therm. Eng.*, vol. 199, no. August, p. 117608, 2021, doi: 10.1016/j.applthermaleng.2021.117608.

[5]   D. A. Saputra, Y. Osaka, T. Tsujiguchi, M. Haruki, M. Kumita, and A. Kodama, "Experimental investigation of desiccant wheel dehumidification control method for changes in regeneration heat input," *Energy*, vol. 205, p. 118109, 2020, doi: 10.1016/j.energy.2020.118109.

[6]   T. S. Ge, Y. J. Dai, R. Z. Wang, and Y. Li, "Performance of two-stage rotary desiccant cooling system with different regeneration temperatures," *Energy*, vol. 80, pp. 556–566, 2015, doi: 10.1016/j.energy.2014.12.010.

[7]   G. Angrisani, F. Minichiello, C. Roselli, and M. Sasso, "Experimental analysis on the dehumidification and thermal performance of a desiccant wheel," *Appl. Energy*, vol. 92, pp. 563–572, 2012, doi: 10.1016/j.apenergy.2011.11.071.

[8]   F. Comino, F. Táboas, F. Peci, and M. Ruiz de Adana, "Detailed experimental analysis of the energy performance of a desiccant wheel activated at low temperature," *Appl. Therm. Eng.*, vol. 178, p. 115580, 2020, doi: 10.1016/j.applthermaleng.2020.115580.

[9]   S. Chai, Y. Zhao, T. Ge, and Y. Dai, "Experimental study on a fresh air heat pump desiccant dehumidification system using rejected heat," *Appl. Therm. Eng.*, vol. 179, no. January, p. 115742, 2020, doi: 10.1016/j.applthermaleng.2020.115742.

[10] J. H. Jacobs, C. E. Deering, R. Sui, K. L. Lesage, and R. A. Marriott, "Degradation of

desiccants in temperature swing adsorption processes: The temperature dependent degradation of zeolites 4A, 13X and silica gels," *Chem. Eng. J.*, vol. 451, no. P4, p. 139049, 2023, doi: 10.1016/j.cej.2022.139049.

[11]   B. Behede, S. Chakrabarti, U. Wankhede, and H. Thakare, "Review on nanoporous inorganic desiccant materials in the context of application in rotary dehumidifiers," *Mater. Today Proc.*, vol. 57, pp. 2174–2179, 2022, doi: 10.1016/j.matpr.2021.12.227.

[12]   C. X. Jia, Y. J. Dai, J. Y. Wu, and R. Z. Wang, "Experimental comparison of two honeycombed desiccant wheels fabricated with silica gel and composite desiccant material," *Energy Convers. Manag.*, vol. 47, no. 15–16, pp. 2523–2534, 2006, doi: 10.1016/j.enconman.2005.10.034.

[13]   K. F. Fong, T. T. Chow, Z. Lin, and L. S. Chan, "Simulation-optimization of solar-assisted desiccant cooling system for subtropical Hong Kong," *Appl. Therm. Eng.*, vol. 30, no. 2–3, pp. 220–228, 2010, doi: 10.1016/j.applthermaleng.2009.08.008.

[14]   S. Misha, S. Mat, M. H. Ruslan, E. Salleh, and K. Sopian, "Performance of a solar assisted solid desiccant dryer for kenaf core fiber drying under low solar radiation," *Sol. Energy*, vol. 112, pp. 194–204, 2015, doi: 10.1016/j.solener.2014.11.029.

[15]   D. B. Jani, *Performance assessment of solar powered hybrid solid desiccant and dehumidification integrated thermally cooling system using TRNSYS*. Elsevier Inc., 2021. doi: 10.1016/b978-0-12-821221-9.00004-9.

[16]   M. M. S. Dezfouli, K. Sopian, and K. Kadir, "Energy and performance analysis of solar solid desiccant cooling systems for energy efficient buildings in tropical regions," *Energy Convers. Manag. X*, vol. 14, no. January, p. 100186, 2022, doi: 10.1016/j.ecmx.2022.100186.

[17]   Y. Li, L. Lu, and H. Yang, "Energy and economic performance analysis of an open cycle solar desiccant dehumidification air-conditioning system for application in Hong Kong," *Sol. Energy*, vol. 84, no. 12, pp. 2085–2095, 2010, doi: 10.1016/j.solener.2010.09.006.

[18]   M. H. Ahmed, N. M. Kattab, and M. Fouad, "Evaluation and optimization of solar desiccant wheel performance," *Renew. Energy*, vol. 30, no. 3, pp. 305–325, 2005, doi: 10.1016/j.renene.2004.04.010.

Chapter 3

Methodology

3.1. Details of the Solar Assisted Desiccant Dehumidification System

The experimental setup of the flat plate solar air collector-assisted desiccant dehumidification system is shown in **Fig.3.1** (a). The rotary desiccant dehumidifier and solar air collector were the primary components of the SADDS. RDW consists of a drum-shaped rotating wheel filled with silica gel to absorb moisture from the process air. It had a porous honeycomb structure that let the air pass out from the desiccant wheel (see **Fig. 3.1** (b)). On each side of the desiccant wheel, two rectangular ducts were attached. The duct's purpose was to maintain the streamlined air flows and prevent the mixing of process and regeneration air flows. Two air blowers with an adjustable flow rate supply air to the process and regeneration channels. Using moisture-retaining material (silica gel), the rotating wheel's process side draws moisture from the surrounding air. By dehumidifying the air with these materials, which have a high-water adsorption capacity, it is possible to achieve the desired relative humidity. As a result, the dehumidification process can cause the wheel to become completely saturated with moisture, necessitating a regeneration process using high heat and dry air to ensure the dehumidification processes can run continuously.

Therefore, heated air was provided for the regeneration of the desiccant material (silica gel) by integrating a FPSAC with the regeneration side inlet of the desiccant system. FPSAC was fabricated inside the lab manufacturing facility. Solar rays from the sun strike the collector, and the collector's highly absorptive surface absorbs thermal energy and transfers it to the air. The collector's interior was insulated with aluminum foil sheets to prevent thermal losses and improve the heat transfer rate between the air and absorber. The air blower was positioned between the FPSAC output and the regeneration side inlet to minimize the volumetric flow rate losses. It draws the hot air from the solar collector and delivers it to the regeneration side inlet. In a SADDS, the process air and the regeneration air were set up to flow in counterflow directions.

At night, the collector does not receive solar energy to regenerate the air; therefore, one electric rod was installed within the regeneration inlet side lid, as shown in **Fig. 3.1** (c). The technical specification of the FPSAC and the RDW is shown in **Table 3.1.**
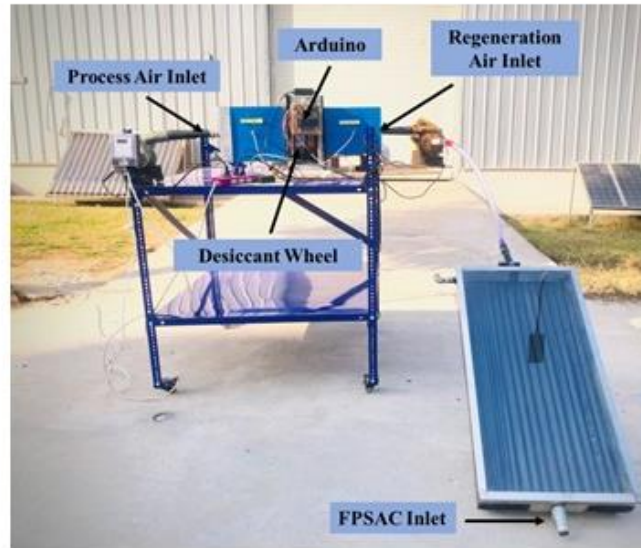
Fig. 3.1 (a) SADDS (b) Desiccant wheel and its internal view (c) Electric rod

Table 3.1. Technical specification of the rotary desiccant dehumidifier and FPSAC

Desiccant Wheel	Rph	104 rev/h
	Rated power	3.75 W
	Wheel dia	254 mm
	Wheel depth	146 mm
	Cassette length/height	350 mm
	Process/ Regeneration air outlet diameter	127 mm
Rectangular Ducts	No. of ducts	4
	Area of each duct	247 mm
FPSAC	Length	1036 mm
	Height	548 mm
	Width	122 mm
	Slope angle	30
	Glazing thickness	5 mm
Process Side Fan	Rated power	600 W
	Rated flow rate	168 m^3/h
Regeneration Side Fan	Rated power	600 W
	Rated flow rate	210 m^3/h
Auxiliary Electric Heater	No. of electric rods	1
	Rated power of rod	400 W

3.2. The Experimental Setup

The prototype of the consolidation of the glazed and unglazed FPSAC and the RDD was assembled and tested in the Emerging Lab of the US-Pak Center of Advanced Studies in Energy at the National University of Science and Technology (NUST), Islamabad in

Pakistan. The proposed system's main novelty was its use of a solar thermal energy by a FPSAC and use of this heated energy for DDS regeneration.

The experimental setup for the SADDS includes the following primary components:

1. The RDW which ensures the dehumidification of the process air and directs it to the process side outlet duct.
2. A flat plate solar air collector that focuses solar radiations coming from the sun, and the air in the collector must be sufficiently heated for desiccant regeneration.
3. Temperature and humidity sensors which monitors data in real time and the data from these sensors was stored on Arduino for process and regenerative air.

Fig 3.2 shows a schematic diagram of the system component integration. To prevent solar thermal radiation from impacting the monitoring data, the FPSAC was installed outside the lab, while the desiccant system was placed inside the lab's entrance. The air blower in the system circulates humid air into the process side inlet duct and directs it to the desiccant wheel; the silica gel inside the honeycomb structure of the wheel absorbs moisture from the air and passes it out to the process side outlet duct (1 → 2). On the other side of the system, solar radiations from the sun were directed on the collector's surface. As a result, the temperature of the air entering the collector gains thermal energy from the absorber plate and rises (3 → 4). The blower drew hot air from the collector and sent it to the regeneration side inlet duct (4 → 5). This heated air eliminates moisture from the wheel surface in readiness for continuous dehumidification and transports moist air from the desiccant wheel chamber to the ambient air (5 → 6).
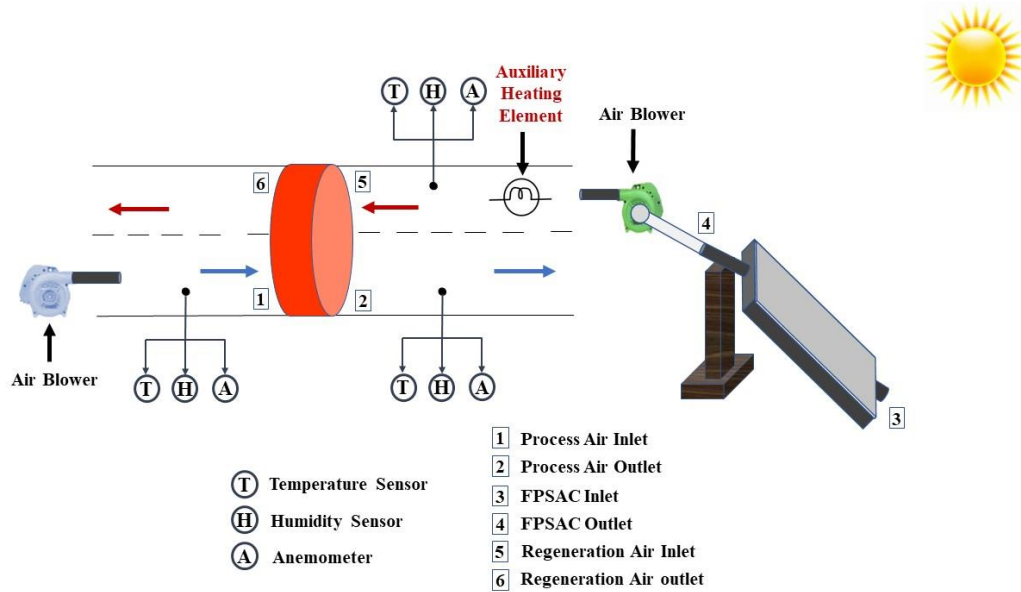
Fig. 3.2 Schematic diagram of FPSAC assisted desiccant dehumidification system

3.3. Test instruments and data acquisition

Air temperature, relative air humidity, and air velocity at the process and regeneration sides were measured in the experiment. The temperature and relative humidity were measured with an accuracy of ±0.5°C and ±2% RH, respectively, using a Nano Arduino (DHT22 sensor). The airflow rate was determined by the cross-sectional area of the rectangular ducts and the air velocity, which was measured using a hot wire anemometer with an accuracy of ±3%. Detailed technical specifications of the measuring instruments are shown in **Table 3.2.**

Table 3.2 Technical specification of the measuring instruments

Parameter	Sensor	Range	Accuracy
Air Temperature	DHT22	-40-80°C	±0.5°C
Air Humidity	DHT22	0-100%	±2% RH
Air Velocity	Hot Wire Anemometer	0-30 m/s	±3%
Global Horizontal Irradiance	Pyranometer	0-1000 W/m^2	±2% W/m^2

3.4. Performance analysis

The proposed system includes two fundamental processes: dehumidification of air employing a RDD and converting solar radiations into thermal energy for desiccant material regeneration utilizing FPSAC. The rate at which moisture was extracted from the air and the temperature at which regeneration occurs in a desiccant dehumidifier are interrelated. As a result, analytical calculations were carried out to assess the effectiveness of the proposed system.

This experimental analysis of the SADDS was carried out under the following simplifying assumptions.

a) There was no air leakage across the rotary desiccant dehumidifier and the glazed FPSAC.

b) Process and regeneration sides are equally divided inside RDW.

The performance of the SADDS system was studied when the regeneration was done with both the glazed and unglazed FPSAC by evaluating the dehumidification effectiveness, a percentage increase in temperature, and moisture removal capacity of the desiccant wheel.

3.4.1. Performance evaluation of FPSAC

In this subsection, the efficiency and useful energy gain of glazed and unglazed FPSAC were computed using mathematical equations.

3.4.1.1. Useful energy gain analysis

Energy gain by the ambient air in the glazed and unglazed FPSAC was calculated as in Eq. (1) [1]:

$$Q_u = m_r \times c_p \times (T_{out} - T_{in})$$
(1)

Where m_r and c_p represent the regeneration air's mass flow rate and specific heat of process air, T_{in} and T_{out} was the air temperature at the FPSAC's inlet and outlet.

3.4.1.2. Thermal efficiency of FPSAC

It is defined as the ratio of the amount of heat energy collected by the solar air collector to the amount of solar radiation incident upon the collector. It was calculated as in Eq. (2) [1]:

$$\eta = \frac{Q_u}{A_c \times I}$$
(2)

Here, Ac represents the FPSAC area, and I symbolize the radiation incident on FPSAC.

3.4.2. Performance analysis of RDD

In this subsection, the following equations were used to assess the performance of DDS when integrated with glazed and unglazed FPSAC.

3.4.2.1. Dehumidification effectiveness

The dehumidification effectiveness (DE) indicates the desiccant wheel's dehumidification capacity. It is the ratio of amount of the moisture removed from the process air by the initial humidity and calculated as in Eq.(3) [2].

$$DE = \frac{\omega_1 - \omega_2}{\omega_1}$$
(3)

3.4.2.2. Percentage increase in temperature

Percentage increase in temperature (% IT) is defined as the increase in temperature of the air after the dehumidification. It was calculated as in Eq. (4).

$$\% \text{ IT} = \frac{T_2 - T_1}{T_1} \times 100 \tag{4}$$

3.4.2.3. Moisture removal capacity

Moisture removal capacity (MRC) shows that the amount of moisture removed by the desiccant wheel per unit time and it was found by Eq. (5)[2].

$$\text{MRC} = \rho_p \times V_p \times (\omega_1 - \omega_2) \tag{5}$$

T_1 - ω_1 and $T_2 - \omega_2$ was the process air's inlet-outlet temperature and relative humidity in the RDW. ρ_p is the inlet process air density.

DE and MRC values that seem higher indicate a more efficient dehumidification process. However, applications that require cooling after dehumidification require a lower % IT value. The cooling load increases considerably as the temperature of the process air outlet gets higher.

3.5. Model validation with TRNSYS Simulation

TRNSYS is a comprehensive simulation software used for modelling and analyzing energy systems. For the purpose of predicting the performance of SADDS and glazed-unglazed FPSAC in terms of the relative humidity of the process air outflow and the temperature of the regeneration intake, a TRNSYS simulation was performed. The studio project was modelled in TRNSYS for the meteorological conditions of Islamabad using the EnergyPlus Weather file (EPW) format. The airflow rates, ambient temperature, and ambient relative humidity, as well as other variables related to the process and the regeneration process, were used as input parameters in developing the TRNSYS model. The primary goal of carrying out the TRNSYS simulation was to validate the simulated results with experimental findings and predict the performance of DDS with glazed and unglazed FPSAC throughout the year.

Fig. 3.3 shows the underlying arrangement of components in a TRNSYS project for a SADDS. **Fig 3.3** (a) illustrates the regeneration integration of DDS with glazed FPSAC, while **Fig 3.3** (b) depicts the regeneration integration of DDS with unglazed FPSAC. The components chosen for creating a system model in the TRNSYS environment were type 1225 used for modelling desiccant dehumidifier, glazed and unglazed FPSAC of type 7c and type 56, respectively, employed for desiccant wheel regeneration, type 925 was used as fans for process and regeneration air flow to the dehumidifier, type 15-3 used for EPW format Islamabad weather file [3], to display the graphical results type 65d selected whereas type 25c was used to print the results in tabulated form.

While incorporating SADDS into the TRNSYS project studio, all of the component characteristics were kept the same as the experimental components, including the fan speed and rated power, collectors' area, and desiccant wheel rated power. **Table 3.3** details the necessary simulation studio components and TRNSYS types for modelling a solar-assisted desiccant dehumidification system.

Table 3.3 List of TRNSYS project studio integrating components

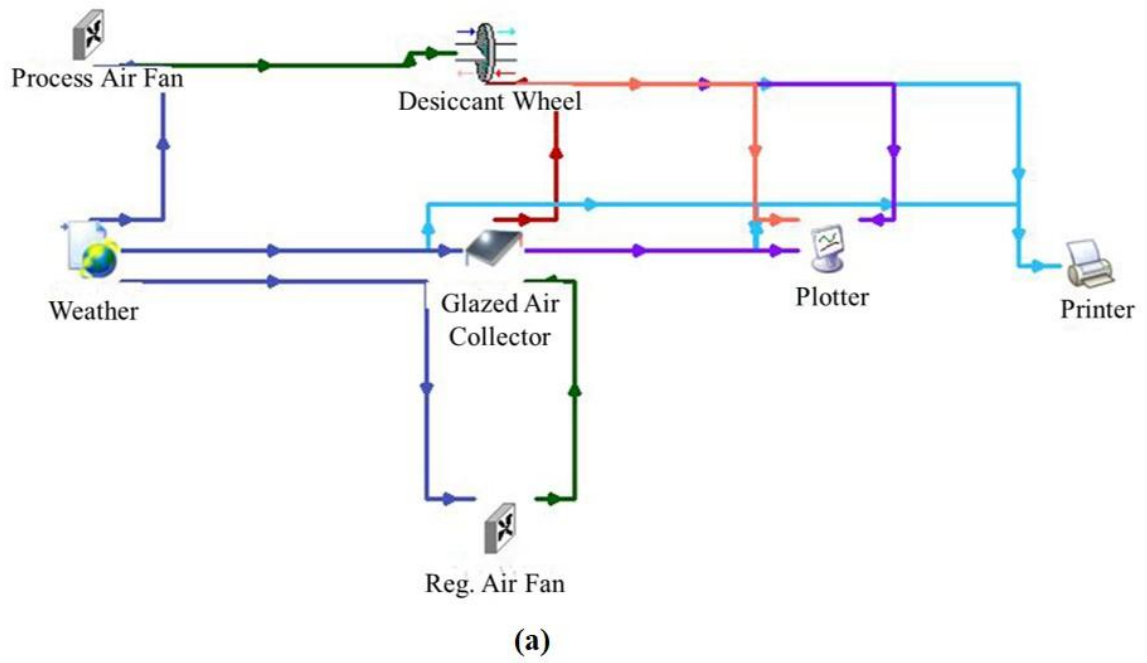| Component	TRNSYS type
Desiccant Wheel	Type 1225
Fan (process air)	Type 925
Fan (regeneration air)	Type 925-2
Glazed FPSAC	Type 7c
Unglazed FPSAC	Type 56
Weather file	Type 15-3
Plotter	Type 65d
Printer	Type 25c
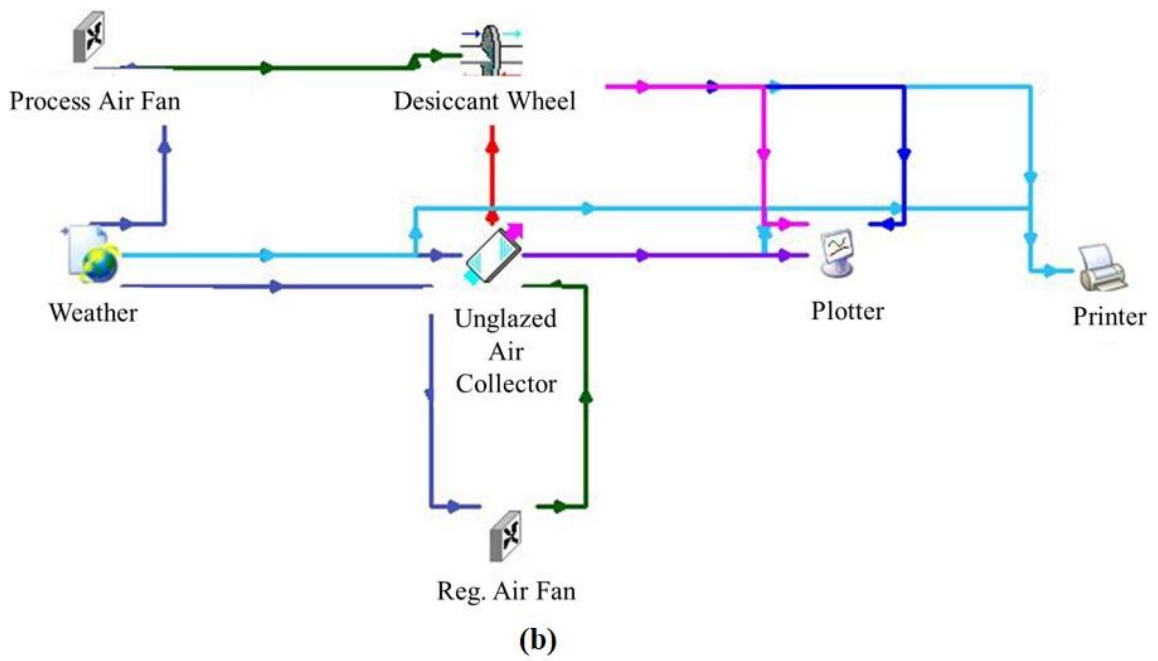
Fig. 3.3 TRNSYS model for DDS with (a) Glazed SAC (b) Unglazed SAC

Summary

This chapter discusses the detailed methodology to complete the experimental setup and simulation model of the SADDS. The experimental setup was tested in a lab, with temperature and humidity sensors to monitor real-time data. The performance of the system was evaluated based on dehumidification effectiveness, temperature increase, and moisture removal capacity. The results were validated through TRNSYS simulations using meteorological data from Islamabad.

References

[1]   M. Ammar, A. Mokni, H. Mhiri, and P. Bournot, "Numerical analysis of solar air collector provided with rows of rectangular fins," *Energy Reports*, vol. 6, pp. 3412–3424, 2020, doi: 10.1016/j.egyr.2020.11.252.

[2]   M. S. Büker, H. I. Parlamis, M. Alwetaishi, and O. Benjeddou, "Experimental investigation on the dehumidification performance of a parabolic trough solar air collector assisted rotary desiccant system," *Case Stud. Therm. Eng.*, vol. 34, no. January, 2022, doi: 10.1016/j.csite.2022.102077.

[3]   "\climatewebsite\WMO_Region_2_Asia\PAK_Pakistan." https://www.climate.onebuilding.org/WMO_Region_2_Asia/PAK_Pakistan/index.html (accessed Mar. 26, 2023).

Chapter 4

Results and Discussion

The FPSAC assisted desiccant dehumidification system was experimentally tested in the month of January for Islamabad climate condition for the duration of 30 minutes. During the tests process-regeneration inlet air relative humidity and temperature was variable and dependent on the ambient conditions. Process inlet air flow rate (33-51-62-m^3/h) were variable while regeneration air flow rate (42 m^3/h) was constant.

In this section, the overall performance of proposed SADDS is discussed in terms of a number of parameters. Since the regeneration process is an important factor to determine the performance of SADDS, preliminary the performances of glazed and unglazed flat plate solar air collector in terms of average collector outlet temperature (T_{out}), average useful energy gain (Q_u)and efficiency have been evaluated in this study.

In addition, the experimental results of desiccant wheel in terms of dehumidification effectiveness (DE), percentage increase in process air outlet temperature (%IT), moisture removal capacity (MRC) for both glazed and unglazed FPSAC have been discussed for three process air flow rates.

4.1. Performance evaluation of glazed and unglazed FPSAC

Experimental examinations were conducted on glazed and unglazed FPSAC. A flow rate of 42 m^3/h was opted to draw performance comparison of glazed and unglazed FPSAC and the results have been plotted in **Fig. 4.1** and **Fig. 4.2**. **Fig. 4.1** presents the T_{out} and Q_u in glazed and unglazed FPSAC. Clearly, it can be assimilated from the experimental results that glazed FPSAC outperforms its corresponding unglazed FPSAC both in terms of T_{out} and Q_u. Glazed FPSAC achieved a maximum T_{out} of 34.33 °C while unglazed FPSAC showed a maximum T_{out} of 32.33 °C. Moreover, Q_u was evaluated to be 762.32 kJ/h and 694.53 kJ/h for glazed FPSAC and unglazed FPSAC respectively.

Fig. 4.2 illustrates the overall thermal efficiency of FPSAC for both glazed and unglazed. Glazed FPSAC showcased an increasing trend with respect to time with a maximum

efficiency of 78.53% as compared to 71.54% for the unglazed. In short, it can be established from these results that glazed configuration of collector yielded the best performance in comparison to its corresponding unglazed collector. This result can be attributed to the phenomenon of greenhouse effect in the glazed FPSAC that allowed more energy absorption in the collector plate which is evident from the useful energy gained (Q_u) by air.

Fig. 4.1 also depicts that Q_u and T_{out} of the air didn't increase after a certain time in both glazed and unglazed FPSAC and eventually achieved a steady-state condition. The reason was that the collector size was small, and the amount of solar radiation that could be absorbed and converted into heat was limited. Thus, a steady-state condition was attained in the heat transfer rate from the collector to the air passing through it. As a result, the air temperature reached a maximum value relatively quickly and then leveled off, even if solar radiation was still available.
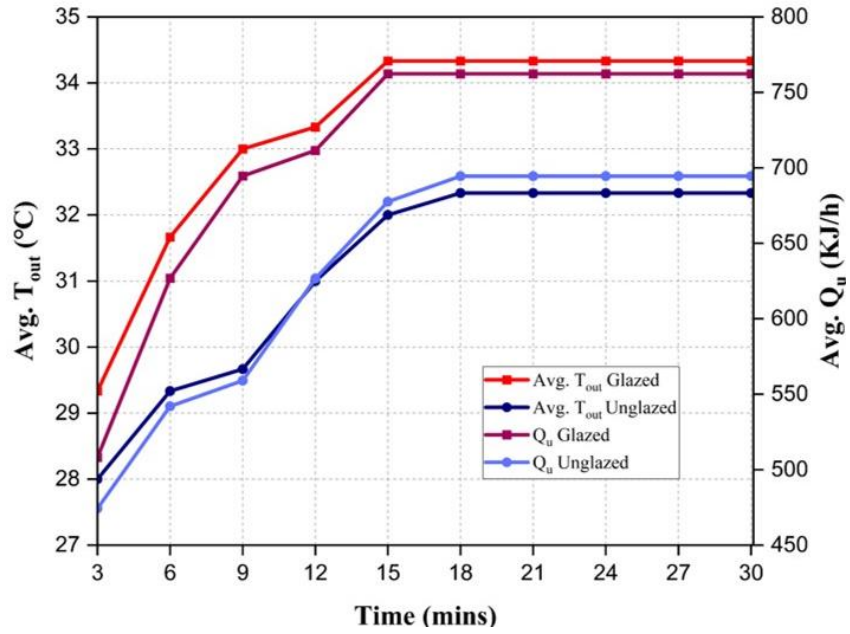
Fig. 4.1 Average outlet temperature (T_{out}) and useful energy gain (Q_u) in glazed and unglazed FPSAC
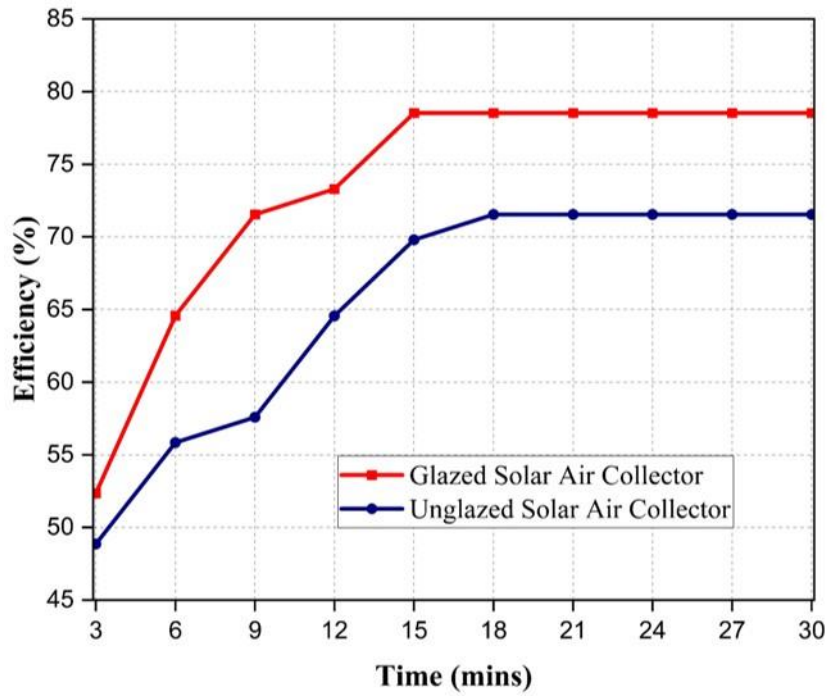

Fig. 4.2 Thermal efficiency of glazed and unglazed FPSAC

## 4.2. Performance Evaluation of Desiccant Wheel

4.2.1. Dehumidification Effectiveness

DE had been experimentally evaluated for both cases when regeneration process was carried out using glazed and unglazed FPSAC for three different process air flow rates (V_p) of 33-51-62-m^3/h. Again, regeneration flow rate (V_r) was kept constant to the value of 42 m^3/h. **Fig. 4.3** (a) depicts the dehumidification effectiveness for the glazed case. It can be assimilated from the graph that DE increased as time increased. In addition, the relationship between DE and flow rate was found to be of inverse in nature. This can be conceptualized from the fact that air with lowest flow rate has more retention time in desiccant wheel as compared to that of with highest flow rate. Therefore, maximum DE was found to be 0.4 at the V_p of 33 m^3/h and the minimum DE was 0.22 at the V_p of 62 m^3/h.

Dehumidification effectiveness for the unglazed case has been presented in the **Fig. 4.3** (b). The experimental outcomes showed that DE for unglazed augmented as the time increased. Moreover, the desiccant wheel having process air regenerated from unglazed FPSACE showed less dehumidification for greater flow rates; a similar behavior to that for glazed case. The results showed a maximum DE of 0.33 at the V_p of 33 m^3/h and the minimum DE of 0.20 at the V_p of 62 m^3/h. However, this dehumidification was slightly less in contrast to the glazed case as the hot air coming from the unglazed collector to the regeneration inlet side of the desiccant system had less temperature as compare to the glazed FPSAC.
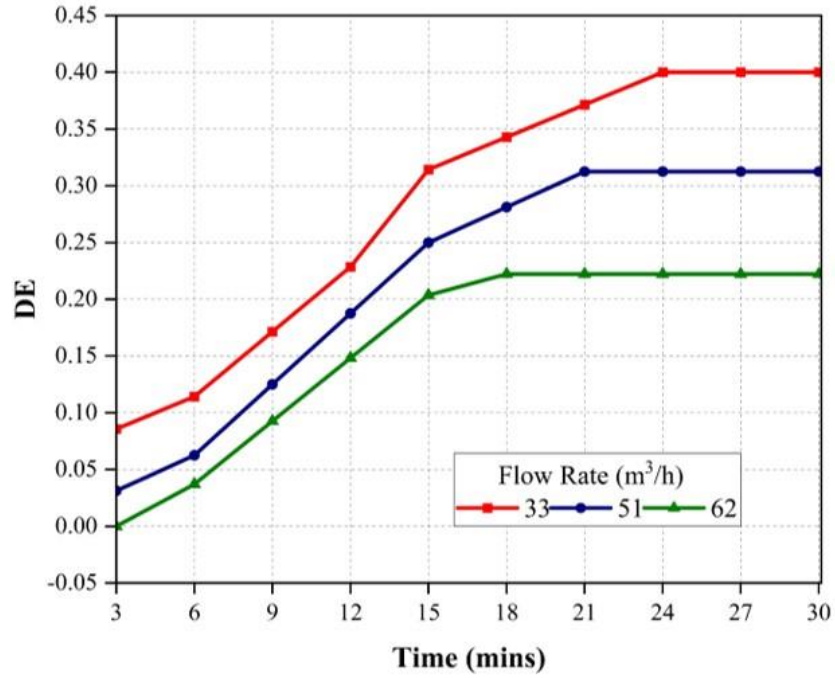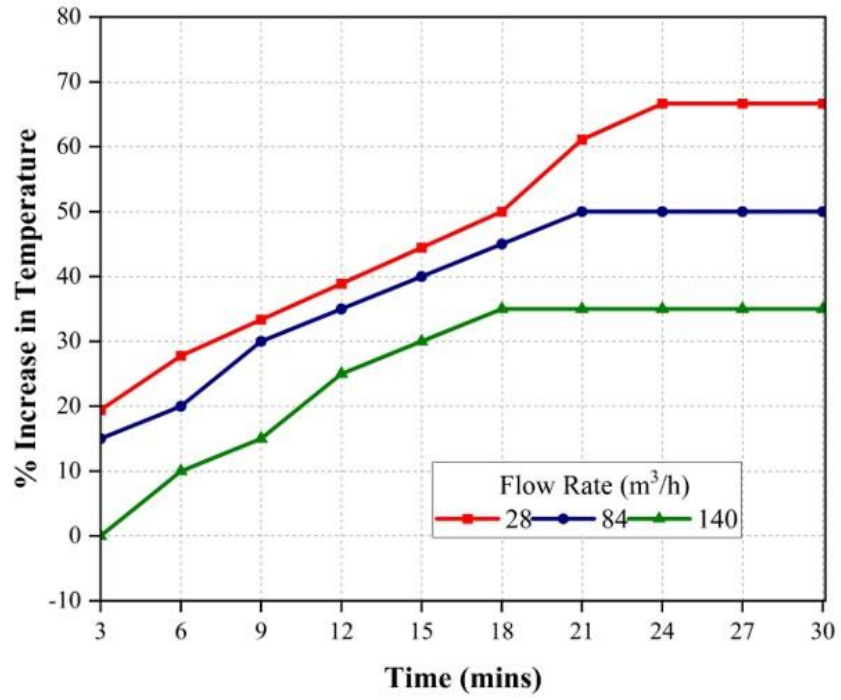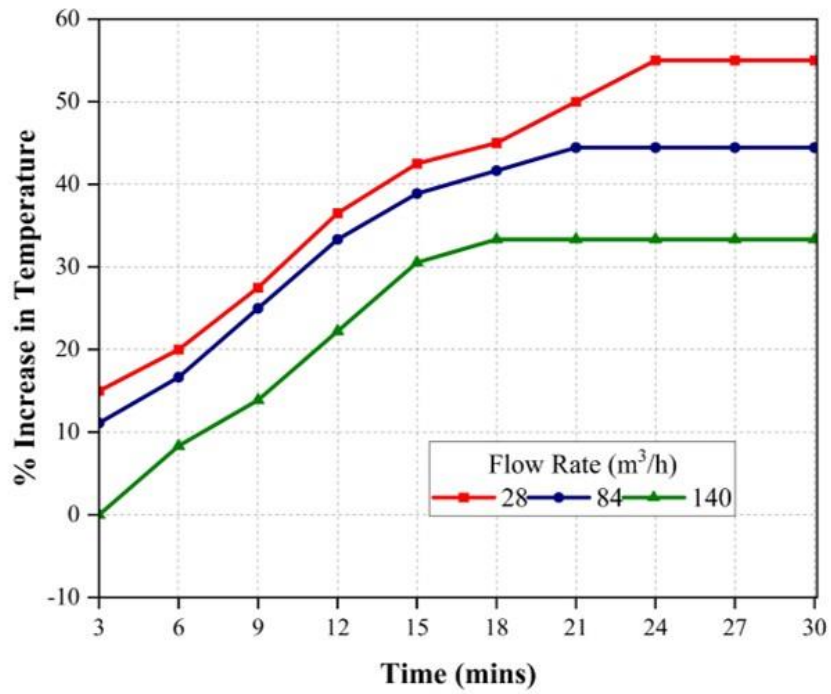
(a)
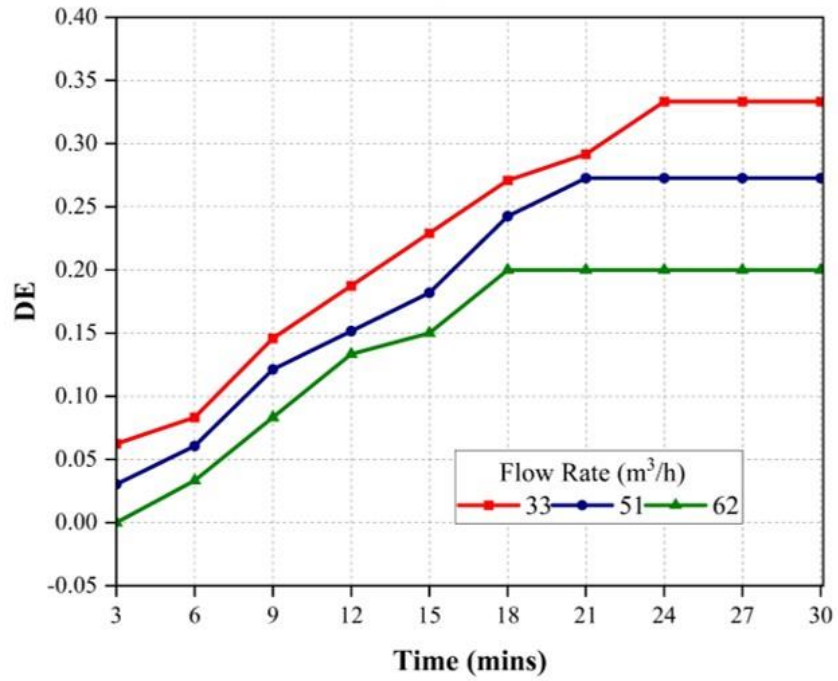
(b)

Fig. 4.3 Dehumidification effectiveness at different flow rates (a) Glazed case (b) Unglazed

Case

4.2.2. Process Outlet Temperature

Fig. 4.4 depicts the air temperature characteristics present at the process side outlet for both glazed and unglazed cases. It can be conceptualized from the graphs that as the air became drier, its temperature increased. In addition, the behavior of air temperature with regard to increasing flow rate is characterized by results that are notably comparable to those of the DE. In simpler words, while the proposed system was operating at the flow rate at which it showed the maximum DE, the output air temperature tends to be greater than when it is operated at higher flow rates. As a result, the maximum percentage increase in temperature for the glazed case was observed to be 66.67% at the V_p of 33 m^3/h, and the minimum percentage increase in temperature was found to be 35% at the V_p of 62 m^3/h (see **Fig. 4.4** (a)). Due to the fact that the DE was lower in the unglazed case in comparison to the glazed case, the percentage rise in temperature in the unglazed case was lower when compared to its counterpart. The maximum percentage increase in temperature was shown to be 55% at the V_p of 33 m^3/h, and the minimum percentage increase in temperature was observed to be 33.33% at the V_p of 62 m^3/h (see **Fig. 4.4** (b)).

Fig. 4.4 Percentage increase in process air outlet temperature (a) Glazed case (b) Unglazed case

4.2.3. Moisture Removal Capacity (MRC)

MRC of the proposed system had been assessed using Eq. (5) and is represented in **Fig. 4.5** for both glazed and unglazed cases. This evaluation was carried out with respect to different flow rates and relative humidities. When compared to the other V_p (33 m^3/h and 62 m^3/h), it was discovered that the V_p of 51 m^3/h resulted in the highest value of the MRC. The information provided by Eq. (5) explains how the MRC depends on flow rates and changes in relative humidity. It was observed that when the airflow rate increased beyond 51 m^3/h, the MRC of the desiccant wheel actually decreased because the air was moving too quickly through the wheel, which reduced the amount of contact time between the air and the desiccant material. Therefore, 33 m^3/h – 51 m^3/h was an optimal range of airflow rates that provided the best balance between dehumidification effectiveness and moisture removal capacity for the proposed SADDS. Maximum MRC was found to be 6.14 kg/h at a V_p of 51 m^3/h for the glazed case (see **Fig. 4.5** (a)), and minimum MRC was found to be 4.47 kg/h at a V_p of 62 m^3/h. For the unglazed case (see **Fig. 4.5** (b)), maximum MRC was found to be 3.57 kg/h at the V_p of 51 m^3/h and minimum MRC was 2.78 Kg/h at the V_p of 62 m^3/h.
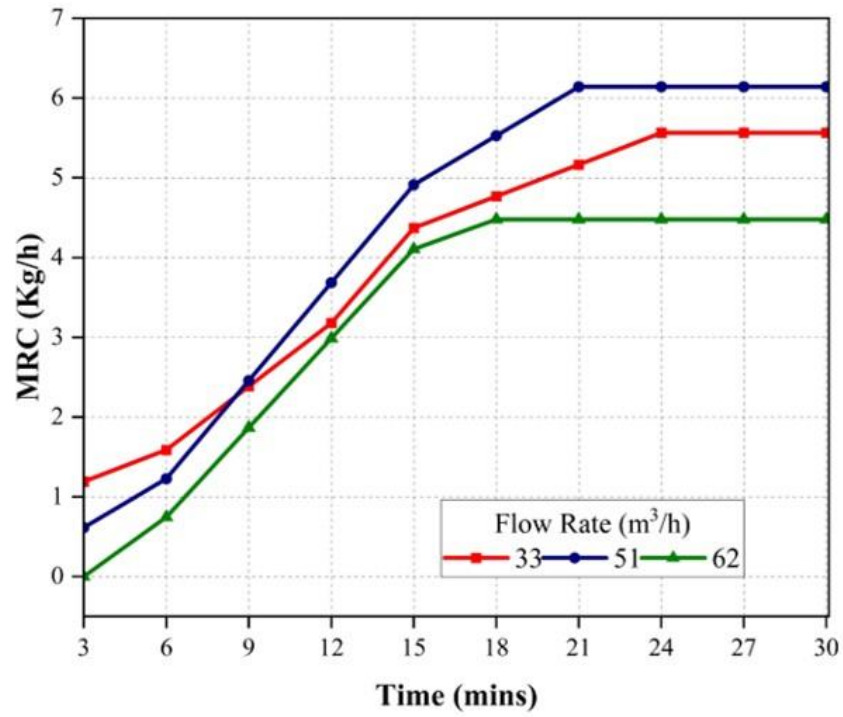
(a)
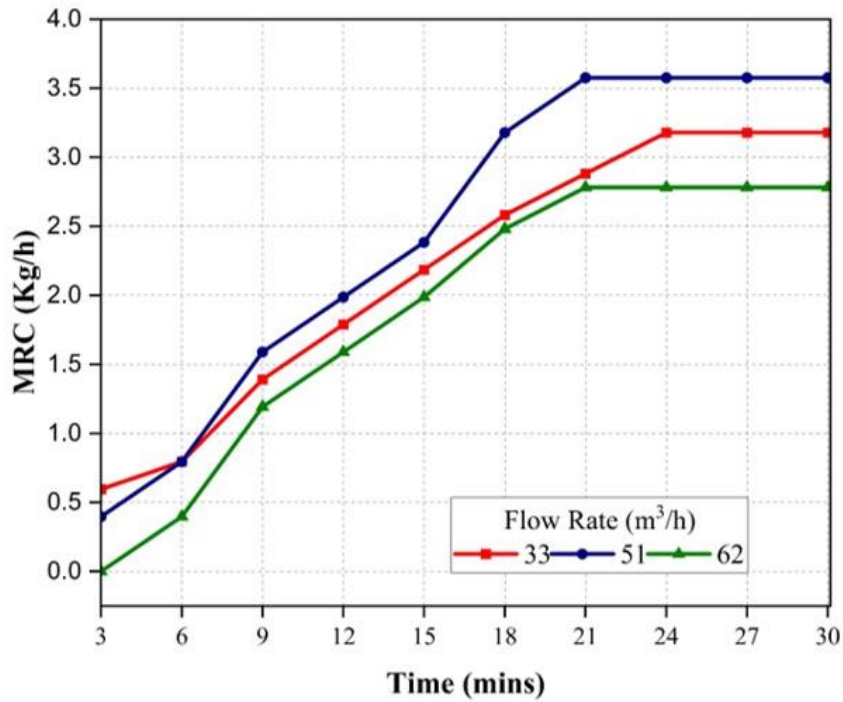
(b)

Fig. 4.5 Moisture removal capacity at different flow rates (a) Glazed case (b) Unglazed case

4.3. TRNSYS Results

TRNSYS was used to simulate SADDS for a period of one year. The simulation was carried out for both glazed and unglazed FPSAC to predict the performance of the proposed system under different weather conditions. V_p and V_r were 33 m^3/h and 42 m^3/h, respectively, and the size of glazed and unglazed FPSAC was 0.567 m^2. To validate the TRNSYS model with experimental data, all integrating component parameters were kept the same as experimental components.

Fig 4.6 represents the performance of DDS with glazed and unglazed FPSAC over the year for Islamabad climatic conditions. Ambient conditions remained same for both glazed and unglazed cases however change in process air outlet humidity and FPSAC outlet temperature for the glazed and unglazed cases can be seen on it.

It is clear from **Fig 4.6** (a) and (b) that the air temperature is higher in the glazed FPSAC compared to its counterpart, unglazed FPSAC. And this effect can also be seen in the process air outlet humidity; in the case of glazed FPSAC, the desiccant system removes more moisture from the air than it does in the case of unglazed FPSAC.
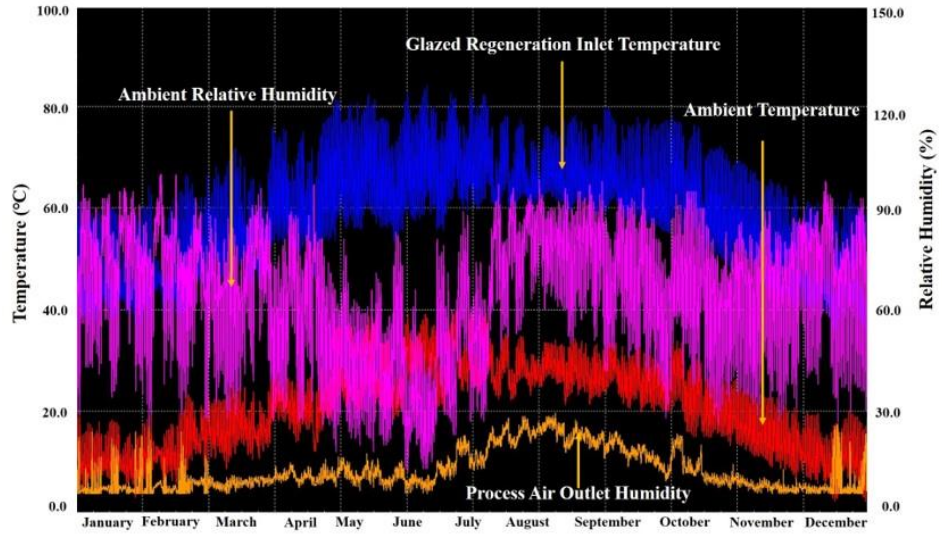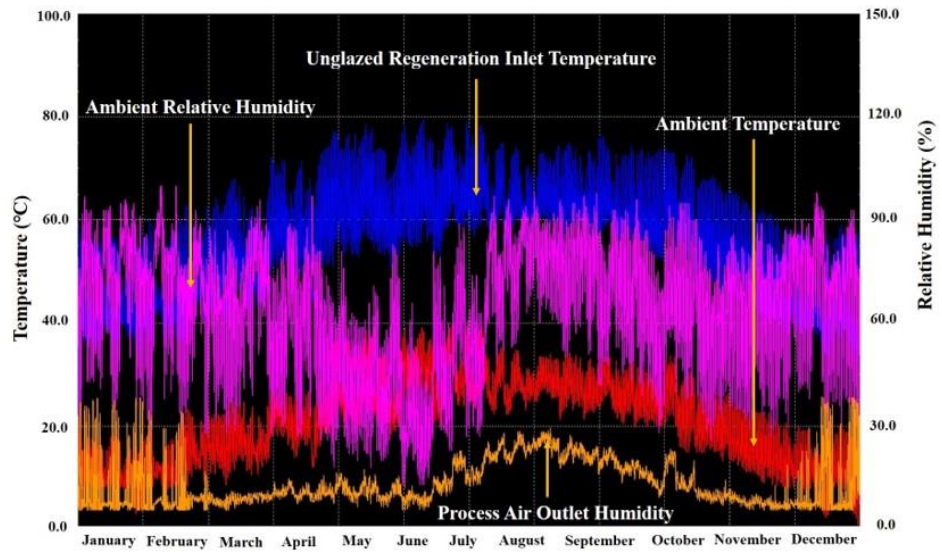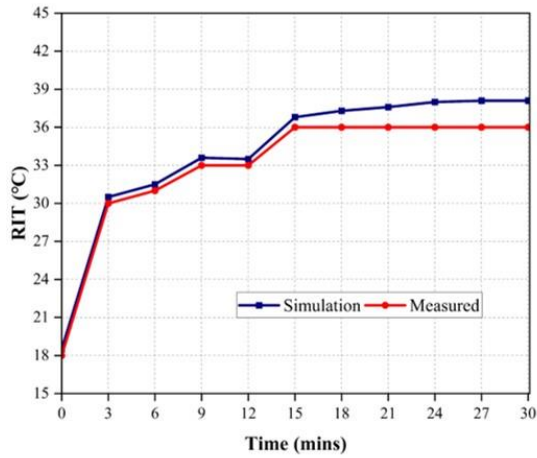
Fig. 4.6 Desiccant dehumidification system with (a) Glazed FPSAC (b) Unglazed FPSAC

4.3.1. Validation of TRNSYS model

Validation of the experimental results in terms of regeneration inlet temperature (RIT), process air outlet humidity (POH) and process outlet temperature (POT) for the DDS for the glazed and unglazed FPSAC regeneration configuration was carried out by comparing with TRNSYS simulation results. Simulation results for glazed FPSAC configuration were evaluated, and the analogy between simulation and experimental results has been drawn in **Fig. 4.7**. RIT, POH and POT have been shown in **Fig. 4.7** (a), (b), and (c), respectively. It was observed from simulated results of RIT, POH, and POT agreed well with the experimental findings and showcased average deviations of 3.2%, 7.2% and 5.9%, respectively.

A similar approach was used to validate the experimental results obtained for unglazed FPSAC, and the analogy between simulation and experimental results has been shown in **Fig. 4.8.** RIT, POH and POT have been shown in **Fig. 4.8.** (a), (b), and (c), respectively. TRNSYS simulation predictions in terms of RIT, POH and POT exhibit average deviations of 6.7%, 3.7%, and 2.9%, respectively.
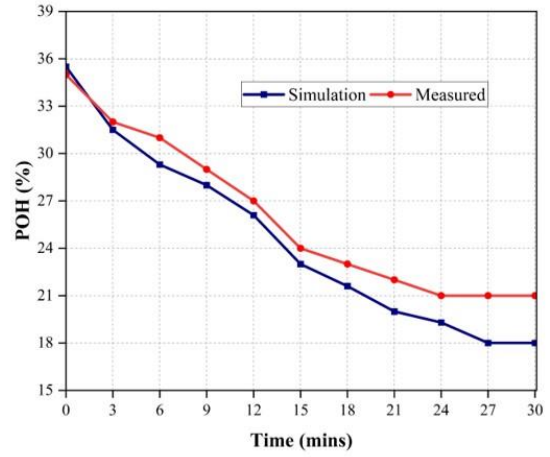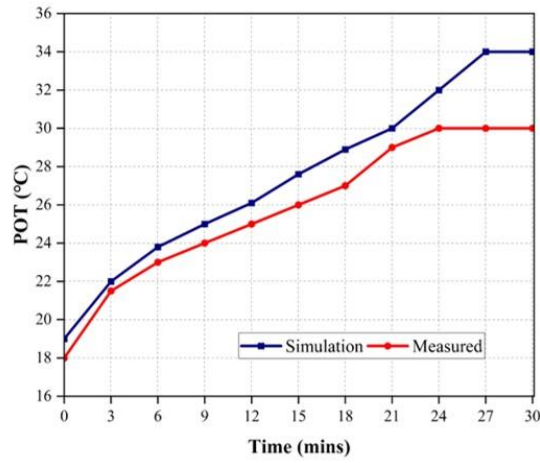
Fig. 4.7 Simulation and measured results of desiccant dehumidification system with glazed FPSAC
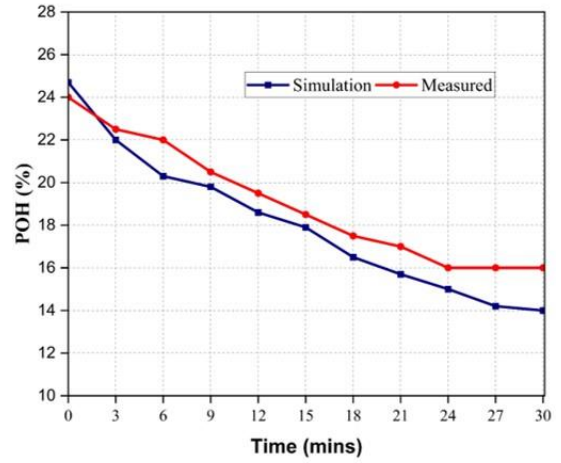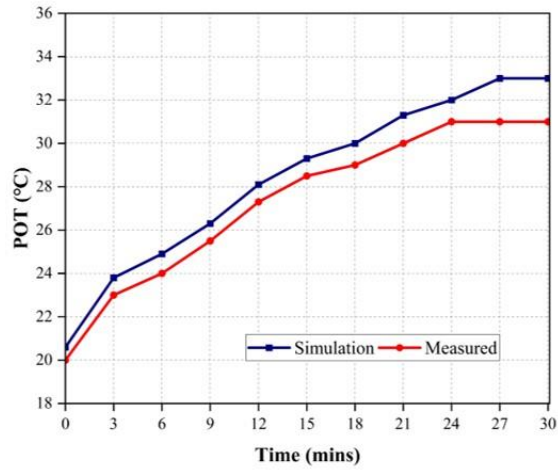
Fig. 4.8 Simulation and measured results of desiccant dehumidification system with unglazed FPSAC

4.4. Environmental Assessment and Financial Analysis

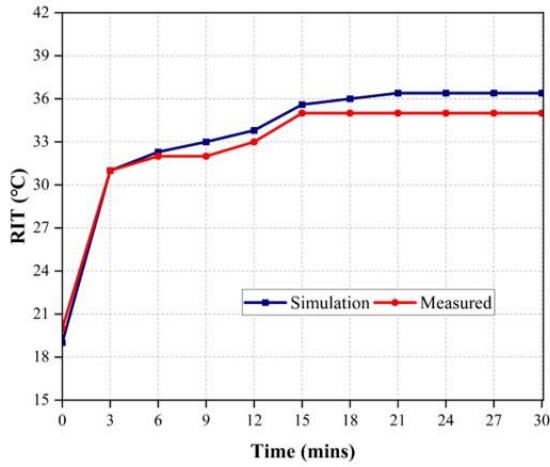The proposed system's components all relied on electricity, except for the regeneration side. On that side, hot air was supplied by the FPSAC rather than an electric rod or an auxiliary heater. Natural gas, Gasoline, Coal and Diesel are the main fuels used in power plants to generate electricity. Natural gas has an ideal calorific value of 40.6 MJ/m^3, gasoline has 34.2 MJ/litre, coal has 30.2 MJ/kg and diesel has 38.6 MJ/litre [1]. Due to losses, ideal calorific value cannot be achieved in actual practice. **Fig 4.9** illustrates the ideal and actual calorific values of different types of fuels when the boiler operates at 85% efficiency.
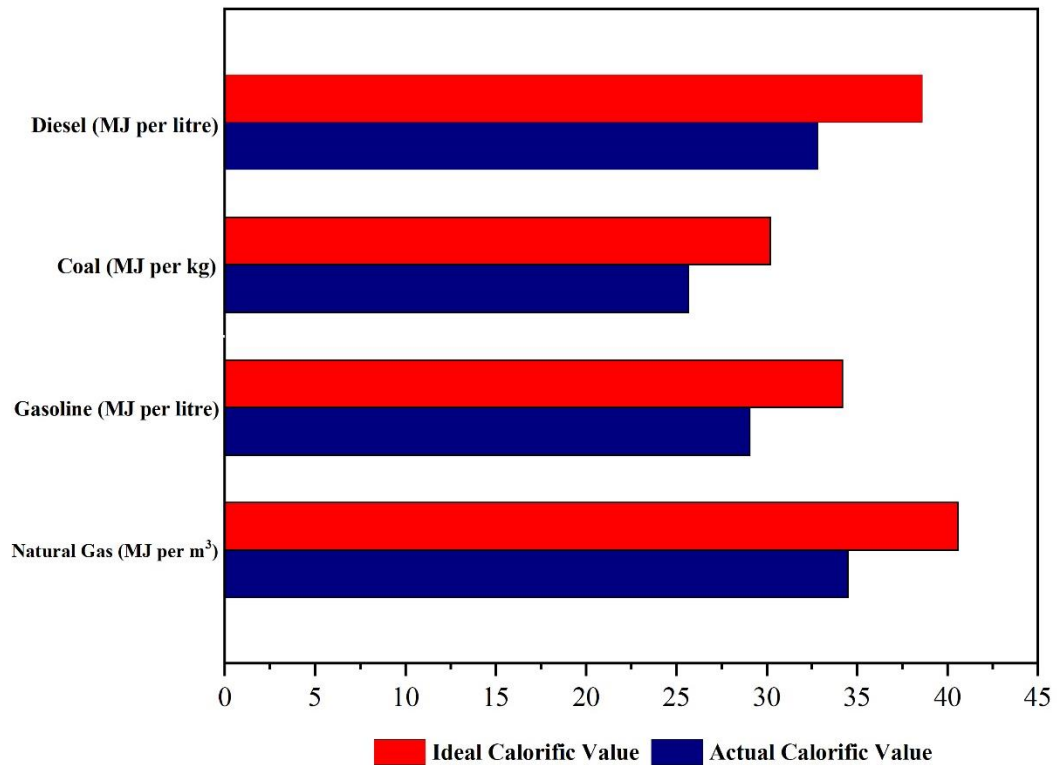
Fig. 4.9 Calorific values of different types of fuels used in the power plant

4.4.1. CO_2 emissions analysis

The significant reduction in greenhouse gas emissions constitutes only a few of the main advantages of using solar collectors to meet the thermal necessities of the systems. In **Fig 4.10**, the red column reflects annual CO_2 emissions from the combustion of conventional fuels to generate electricity for the DDS with an auxiliary electric rod. In contrast, the blue column demonstrates that CO_2 emissions are decreased when the solar hybrid system of desiccant dehumidification system opts for dehumidification.

Fig. 4.10 Annually CO2 emission by burning of different fuels to run DDS

4.5. Solar Fraction

Solar fraction (SF) is the heat energy that the FPSAC gets from the sun as a proportion of the total energy the system needs and Eq. (7)[2] was used for calculating the SF of the proposed system.

$$SF = \frac{\text{Energy delivered by collector}}{\text{Total energy}} \times 100 \qquad (6)$$

Since FPSAC cannot regenerate the desiccant system at night, an auxiliary electric rod will be used at time night for continuous dehumidification. Islamabad, Pakistan, sees an average of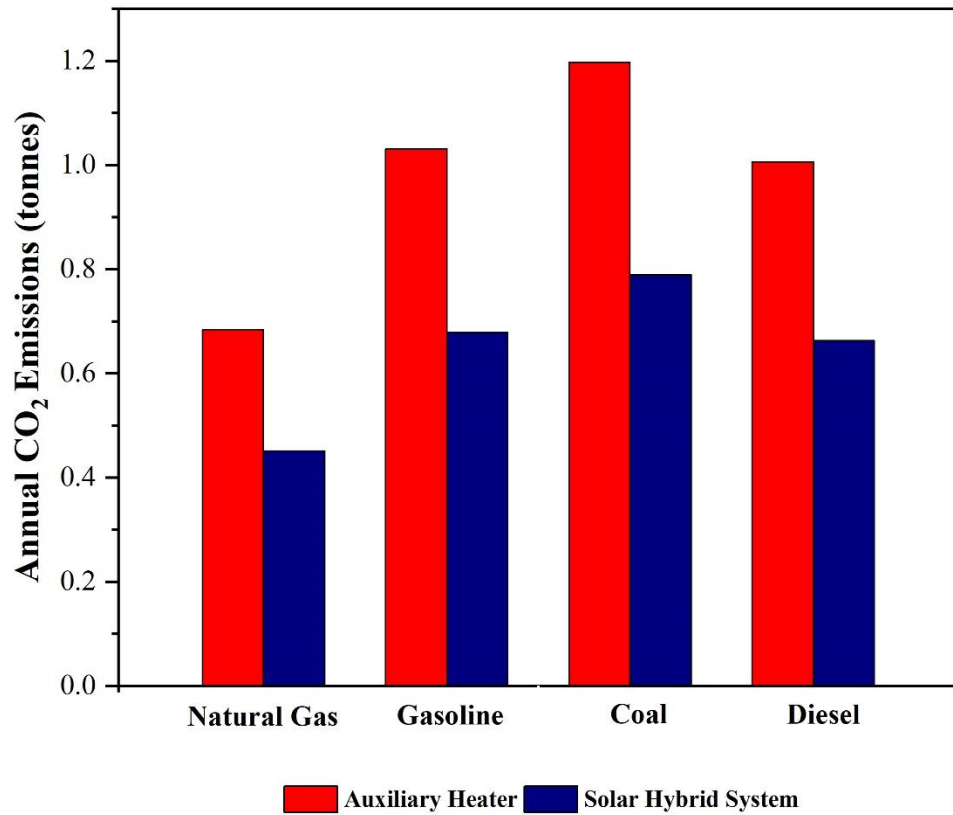 2,945 hours of sunlight annually [3]. So, the SF for the regeneration side of the proposed solar hybrid system would be 33.57%.

4.6. Financial Analysis

One of the most important steps in performing an economic analysis of a project is determining the costs, including the costs of necessary equipment. The costs in this study can be divided into two categories: initial costs and annual operations and maintenance (O&M) costs. The initial cost on the proposed system is shown in a **Table 4.1**. O&M costs include maintenance and repairing cost of the components and it is taken in between 1-3% of the total initial investment [4]. For the proposed system it was taken 2%. The total capital cost of the proposed system is shown in Table **4.2.**

Table 4.1 Initial cost of the proposed system

Equipment/Job	Quantity/ size	Cost Per Unit ($)	Total cost ($)
Desiccant system modification	1	140	140
Flat plate solar air collector	0.567 m^2	200	200
Air blowers	2	40	80
Ducts	4	14	56
Electric rods	1	2	2
Data measuring instruments	2	300	300
Collector field preparation cost (10% of the total cost)[4]			6.38
Total initial investment			784.38

Table 4.2 Total cost of the proposed system

Technology	Initial cost ($)	Annual O&M ($)	Total capital cost ($)
FPSAC	784.38	15.68	800.06

The obtained information is then used to find the payback period of the proposed system. Eq. (7) [5] was used for calculating the payback period of hybrid system.

$$\text{Payback Period} = \frac{\text{Total capital cost}}{\text{Annual cash flow}} \qquad (7)$$

The average price of natural gas is 0.8755\$/m^3, gasoline is 1.35 \$/litre, diesel is 1.28\$/litre, gasoline is 1.41\$/litre [6] and coal is 0.14 \$/kg [7]. The amount of fuel and cost savings by the integration of a solar hybrid DDS and the payback period of the system by using different types of fuels are shown in **Table 4.3**.

Table 4.3 Fuel and cost saving and payback period of the proposed system by using different fuels

Fuel	Fuel saving	Cost saving ($)	Payback period
Natural gas	125.47 m^3	109.84	7.28 years
Gasoline	148.95 litres	201.083	3.97 years
Coal	168.67 kg	23.61	33.88 years
Diesel	131.97 litres	168.92	4.73 years

Summary

This chapter discusses the experimental results of glazed and unglazed SADDS in terms of DE, Percentage increase in temperature and MRC. TRNSYS simulation model validated with experimental results in both glazed and unglazed cases. Moreover, carbon emission and financial assessment is also done in this chapter.

References

[1]   "Fuels - Higher and Lower Calorific Values." https://www.engineeringtoolbox.com/fuels-higher-calorific-values-d_169.html (accessed Mar. 30, 2023).

[2]   M. M. S. Dezfouli, K. Sopian, and K. Kadir, "Energy and performance analysis of solar solid desiccant cooling systems for energy efficient buildings in tropical regions," *Energy Convers. Manag. X*, vol. 14, no. January, p. 100186, 2022, doi: 10.1016/j.ecmx.2022.100186.

[3]   "Islamabad climate: weather by month, temperature, precipitation, when to go." https://www.climatestotravel.com/climate/pakistan/islamabad (accessed Mar. 31, 2023).

[4]   U. Eicker, D. Schneider, J. Schumacher, T. Ge, and Y. Dai, "Operational experiences with solar air collector driven desiccant cooling systems," *Appl. Energy*, vol. 87, no. 12, pp. 3735–3747, 2010, doi: 10.1016/j.apenergy.2010.06.022.

[5]   M. W. Kareem, K. Habib, M. H. Ruslan, and B. Baran, "Thermal performance study of a multi-pass solar air heating collector system for drying of Roselle (Hibiscus sabdariffa)," *Renew. Energy*, vol. 113, pp. 281–292, 2017, doi: 10.1016/j.renene.2016.12.099.

[6]   "Gasoline and diesel prices by country | GlobalPetrolPrices.com." https://www.globalpetrolprices.com/ (accessed Mar. 31, 2023).

[7]   "Coal PRICE Today | Coal Spot Price Chart | Live Price of Coal per Ounce | Markets Insider." https://markets.businessinsider.com/commodities/coal-price (accessed Mar. 31, 2023).

Chapter 5

Conclusions and Future Recommendations

5.1. Conclusion

The performance of a solar-assisted desiccant dehumidification system with a glazed and unglazed flat plate solar air collector under different process air flow rates was studied in this study. The study was conducted in a lab-scale environment to account for the climatic conditions in Islamabad, Pakistan. Based on the results of the experiments, the effectiveness of the dehumidifier, the percentage of temperature increase, and the amount of moisture removed were analyzed. To ensure that the simulated results agreed with the experimental findings, the TRNSYS model was developed. The main conclusions from this study are summarized as follows:

- The experimental results indicated that glazed FPSAC integrated DDS performs better as compared to its counterpart in all performance evaluation parameters.
- Both glazed and unglazed integrated DDS showed their maximum dehumidification effactiveness and percentage increase in temperature at the V_p of 33 m^3/h. The glazed case achieved a maximum dehumidification efficiency of 0.4 and a temperature increase of 66.67%, while the unglazed case achieved a maximum dehumidification effectiveness of 0.33 and a temperature increase of 55%.
- At a V_p of 51 m^3/h, the maximum moisture removal capacity for glazed and unglazed cases was determined to be 6.14 kg/h and 3.57 kg/h.
- The TRNSYS model agreed well with the experimental results for glazed and unglazed FPSAC-assisted DDS.
- For the solar hybrid DDS, the solar air collector's solar fraction was 33.57%, and the annual CO_2 emissions for the gasoline fuel will be reduced to 0.352 tonnes.

- The annual energy saving for the solar hybrid DDS will be 1.175 MW with a payback period of 3.97 years for gasoline fuel.

5.2. Experimental Limitations and Future Recommendations

As an alternative to conventional dehumidification methods, SADDS was developed. However, some experimental limitation was placed on this system, which is discussed below.

1. The experimental prototype was design for a lab-scale; therefore, the operating capacity of the components was limited.

Future research could consider integrating PV panels with other parts of a SADDS to power the entire system with renewable energy. In addition, the dehumidified air from the SADDS can be cooled using a direct or indirect evaporative cooler, making it suitable for use in both domestic and industrial sectors.

Acknowledgment

All praise and gratitude be to Allah, the Almighty, who endowed me with the ability to grasp, learn, and finish my thesis report.

I would like to take this opportunity to offer my heartfelt appreciation to my supervisor, Dr. Mariam Mahmood, for her invaluable insights, knowledge, and support over the course of this project. I would also like to acknowledge Dr. Adeel Waqas, Dr. Majid Ali, Dr. Mustafa Anwar and Sir Qamar-ud-Din for guiding me throughout the project. Moreover, I would also like to thank my family and friends, particularly Muhammad Haroon Iqbal, Sabooh-ul-ain, Zoneera Asif, Haseeb Khalid and Chaudhary Abdullah, for their constant motivation and support.

Appendix I: Research Article

Title

Techno-Economic and Emission Analysis of Solar Assisted Desiccant Dehumidification System: Experimental and Numerical Approach

Abstract

In humid climates, it is challenging to maintain the amount of moisture content in the air for human thermal comfort and industrial applications. Regeneration is an essential process during moisture removal through a desiccant dehumidifier. Commercial desiccant dehumidifiers rely on conventional electric heaters to regenerate desiccant material, accounting for significant energy consumption by such systems. As a green solution to this problem, the present study integrates a flat plate solar air collector (FPSAC) with a desiccant dehumidifier to effectively use solar thermal energy and reduce electrical consumption. Performance evaluation of glazed and unglazed FPSAC-assisted desiccant dehumidifier has been conducted at process air flow rates of 33, 51 and 62 m^3/h with a constant regeneration flow rate of 42 m^3/h. Both glazed and unglazed FPSAC assisted desiccant dehumidification systems had the highest dehumidification effectiveness and percentage increase in temperature at the flow rate of 33 m^3/h, while the highest moisture removal capacity was at 51 m^3/h. Maximum dehumidification effectiveness, percentage temperature increase, and moisture removal capacity for the glazed case were 0.4, 66.67%, and 6.14 kg/h, respectively. Experimental results showed that the glazed FPSAC-integrated desiccant dehumidification system outperforms its counterpart in all performance evaluation parameters. Using Transient System Simulation software (TRNSYS), the proposed glazed and unglazed assisted desiccant dehumidification system was modeled and validated with experimental results in terms of regeneration inlet temperature, process air outlet relative humidity, and process air outlet temperature at a flow rate of 33 m^3/h. Furthermore, a techno-economic analysis of the solar hybrid desiccant dehumidification system has been carried out. The FPSAC used in this study showcased a 33.57% yearly solar fraction with a solar hybrid system having a payback period of 7.28 years with gasoline as a fuel source for auxiliary energy. In addition, the

62

hybrid system can reduce greenhouse gas emissions yearly by about 0.352 tonnes of CO_2 equivalents.

Journal Name

Sustainable Energy Technologies and Assessments (Submitted)

Authors

Wasif Iqbal, Mariam Mahmood, Adeel Waqas, Naveed Ahmed, Muhammad Haroon Iqbal

Appendix II: Conference Article

Title

Performance Evaluation of Solar Air Collector Assisted Desiccant Dehumidification System

Abstract

Recently, a considerable growth in energy demand has been observed and predominantly this increased demand in energy is met by the burning of fossil fuels. Renewable forms of energy can offer solutions to issues that have persisted for a long time in the energy sector. Most promising form of renewable energy is solar energy and solar air collectors are an effective technique of utilizing abundant solar energy for heating purposes and lowering the consumption of electrical energy and fossil fuels. This study integrated a flat plate solar air collector with desiccant dehumidification system to regenerate desiccant material. The performance of the proposed FPSAC-assisted rotary desiccant system in terms of outlet temperature, dehumidification effectiveness (DE), moisture removal capacity (MRC) and sensible energy ratio (SER) was evaluated by varying flow rates of process air in the range 33 m^3/h, 51 m^3/h, and 62 m^3/h. The experimental results indicate that an inlet process air flow rate of 33 m^3/h provides the maximum DE (0.71) and the maximum percentage increase in air temperature (68.42%) after dehumidification. Furthermore, highest MRC and SER values were found to be to 12.69 kg/h and 1.26 for the highest process air inlet flow rate i.e., 62 m^3/h. In short, this study provides information on the potential of a FPSAC to provide regeneration air for continuous desiccant dehumidification.

Conference Name

Authors

Wasif Iqbal, Mariam Mahmood, Adeel Waqas, Majid Ali, Naveed Ahmed, Muhammad Haroon Iqbal